AN INVESTIGATION AND CHARACTERIZATION OF A HIGH ENERGY
PIEZOELECTRIC PULSE GENERATOR

A Thesis presented to the Faculty of the Graduate School
University of Missouri- Columbia

In Partial Fulfillment
Of the Requirements for the Degree

Masters of Science

By

CAROLINE SUSAN PINKSTON

Dr. Thomas G. Engel, Thesis Supervisor

DECEMBER 2005

The undersigned, appointed by the Dean of the Graduate School, have examined the thesis entitled

INVESTIGATION AND CHARACTERIZATION OF A HIGH ENERGY
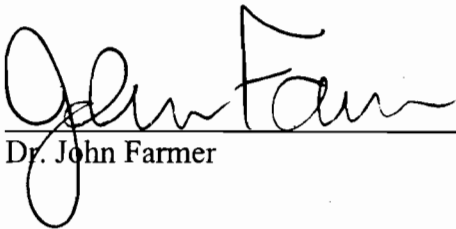PIEZOELECTRIC PULSE GENERATOR

Presented by Caroline Susan Pinkston

a candidate for the degree of Masters of Science in Electrical Engineering

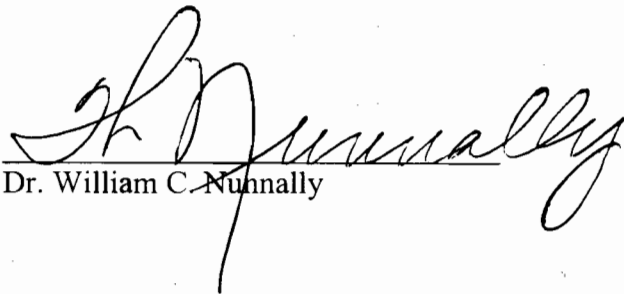and herby certify that in their opinion it is worthy of acceptance.

Dr. Thomas G. Engel (chairman)

Dr. John Farmer

Dr. John Gahl

Dr. William C. Nunnally

INVESTIGATION AND CHARACTERIZATION OF A HIGH ENERGY
PIEZOELECTRIC PULSE GENERATOR

Caroline Susan Pinkston

Dr. Thomas G. Engel, Thesis Supervisor

ABSTRACT

This research investigates and characterizes a high energy piezoelectric pulse generator (PPG) constructed from commercially available piezoelectric materials. The high energy PPG converts mechanical energy into electrical energy, storing that energy in its internal capacitance. The energy storage of the high energy PPG developed here is more than an order of magnitude greater compared to previous investigations [1-2]. The large internal capacitance in the high energy PPG is created by stacking numerous single-element piezoelectric devices and electrically connecting them in parallel. The total internal capacitance of the PPG is around 0.15 μF. The high energy PPG is piezoelectrically charged to greater than 1 kV, thereby storing 50 mJ. The mechanical force needed to compress is derived from a steel mass. The high energy PPG uses a variable height and neoprene material to control the force. Peak forces around 18 kN are used to compress the piezoelectric material. An electromechanical model of the PPG is developed in PSpice and used to predict the performance of the high PPG under a variety of conditions. The PSpice simulations are compared to experimental test results with mechanical force rise-times ranging from sub-millisecond to several milliseconds. There is good agreement between the theoretical predictions and experimental result. The experimental research of the high energy PPG uses a variety of conditions to characterize the system of the high energy PPG.

NOMENCLATURE

$A_{compress}$	Surface area of neoprene material	Meter^2
A_{piezo}	Surface area of piezoelectric material	Meter^2
C	Energy storage capacitance	Farad
C_{stack}	Piezoelectric stack capacitance	Farad
$c_{compress}$	Damping constant of neoprene material	Newton-Second/Meter
c_{piezo}	Damping constant of piezoelectric material	Newton-Second/Meter
E	Energy storage of system	Joule
f	Resonant frequency	Hertz
F	Input force from compression mass	Newton
f_{max}	Maximum impedance frequency	Hertz
f_{min}	Minimum impedance frequency	Hertz
K_{33}	Piezoelectric coupling factor	Dimensionless
$k_{compress}$	Spring constant of neoprene material	Newton/Meter
k_{piezo}	Spring constant of piezoelectric material	Newton/Meter
l	Width of material	Meter
l_{piezo}	Width of piezoelectric material	Meter
$m_{forcemass}$	Compression mass	Kilogram
m_p	Piezo element mass	Kilogram
$m_{compress}$	Neoprene material mass	Kilogram
m_{piezo}	Piezoelectric stack mass	Kilogram
m_{ppg}	System mass	Kilogram
$r_{compress}$	Neoprene material radius	Centimeter
r_{piezo}	Piezoelectric material radius	Centimeter
R_{Loss}	Loss resistance of piezoelectric material	Ohm
V	Output Voltage	Volt
V_{max}	Maximum Voltage	Volt
$V_{poling\ field}$	Poling field Voltage	Volt
V_{stack}	Stack voltage	Volt
W_{mech}	Mechanical energy generated from the input force	Joule
w_{piezo}	Thickness of piezoelectric element	Meter
x_c	Compression distance of neoprene material	Meter
$x_c{}'$	Compression velocity of neoprene material	Meter/Second
$x_c{}''$	Compression acceleration of neoprene material	Meter/Second^2
x_p	Compression distance of piezoelectric material	Meter
$x_p{}'$	Compression velocity of piezo material	Meter/Second
$x_p{}''$	Compression acceleration of piezo material	Meter/Second^2
ε_o	Permittivity in free space	Dimesionless
ε_r	Relative permittivity of material	Dimensionless
δ	Piezoelectric dissipation factor	Dimensionless
$\rho_{compress}$	Density of neoprene material	Kilogram/Meter^3
ρ_{piezo}	Density of piezoelectric material	Kilogram/Meter^3
τ	Time constant	Seconds
ω	Angular frequency	Radian/Second

ABBREVIATIONS

APC	American Piezo Company
LEMD	Lumped Element Mechanical Device
MEMS	Microelectromechanical Structure
PIEZO	Piezoelectric
PPG	Piezoelectric Pulse Generator
PVC	Polyvinyl Chloride
PZ	Piezoelectric
PZT	Lead Zirconate Titanate

TABLE OF CONTENTS

LIST OF FIGURES

LIST OF TABLES

Table

Chapter 1 Introduction

In today's society, there is an ever increasing need for additional sources of energy and power. One such need is for a high energy Piezoelectric Pulse Generator (PPG). The use of piezoelectric materials reduces the need for batteries or other sources of primary power, thus producing less waste. Another benefit is the efficiency of energy transfer of piezoelectric materials is relatively high. A high energy PPG can be used for such applications as laser pumping, electron beam, rail gun, plasma research, landmine detection device, igniter, and others [1]. The industries and technical disciplines use piezoelectric ceramics for alarms, lasers, ink jet printing, sonar, gyros, hydrophones and gas fired equipment such as a barbeque grill [2].

Piezoelectricity was first discovered by Pierre and Jacques Curie in the 1880's. They found that in asymmetrical crystals possessing a polar axis, the effect of a compression parallel to the polar axis was to polarize the crystal, resulting in the generation of a positive charge on one side of the material and a negative charge on the other side of the material. Piezoelectricity is defined as a property of certain classes of crystalline materials or in simple terms "pressure electricity". The crystalline materials or ceramics, for example, include quartz, Rochelle salt, tourmaline, and barium titanate, and zirconate titanate (PZT). Electricity is developed when pressure is applied to one of these materials. When an electric field is applied to the material, the crystal changes shape. The materials do not have piezoelectric properties in their original state. Piezoelectric behavior is induced in these materials by a polarizing treatment referred to as poling [2]. The direction of the polarity on the piezo material is dependent on the poling field. The poling process permanently

changes the dimensions of a ceramic. After the poling process is completed a compressive force is applied to the ceramic element to generate a voltage.

Several recent studies have investigated piezoelectric power generation. One study used lead zirconate titanate (PZT) wafers in shoes to convert mechanical walking energy into usable electrical energy. This system's proposed use was to provide 1.3 mW at 3V when walking [3]. Other projects propose the use of piezoelectrical generators to extract electrical energy from mechanical vibration in machines to power MEMs devices. This work extracted a very small amount of power ($< 5\mu W$) from the vibration and no attempt was made to store the energy [3]. A recent medical application has proposed the use of a piezoelectric generator to promote bone growth. It uses an implanted bone prosthesis containing a piezoelectric generator configured to deliver electric current to specific locations around the implant. It also uses unregulated energy and it is not clear whether the technique has passed beyond the conceptual phase [3]. Yet another development of a piezoelectric generator was performed by Engel as the source for landmine detection in 1996 [1]. One particular investigation shows the peak power output of the experimental generator ranging from 7 to 28 kW. The investigation also shows that maximum peak power scales with increasing piezoelectric material's volume. The work uses piezoelectric materials to convert kinetic energy into a spark to detonate an explosive projectile on impact [4]. Although all of these studies have had success in extracting power from piezoelectric elements, the issues of conditioning and storage were never addressed. In the investigation of the high energy electric piezoelectric pulse generator (PPG) it is characterized and modeled after these previous studies but has

2

gained success in storage of the electrical energy from the piezoelectric elements and reaching a magnitude higher in generating electrical power.

In this case of the high energy PPG, the main concept is to convert mechanical energy into electrical energy using piezoelectric materials. The PPG is constructed from commercially available materials and the conversion of mechanical energy into electrical energy is accomplished by storing energy in the internal capacitance of the piezo material. The energy storage discussed and developed in this exploration is an order of magnitude greater than in the previous studies discussed. In this analysis, the high energy PPG is piezoelectrically charged to 1000 volts or greater. The internal capacitance is charged to 0.15 µF and the external capacitance to 0.1 µF, thereby storing nearly one joule of total output energy for a minimum of 5 seconds. In this analysis of the high energy PPG, the charge was stored for a total of 10 seconds. The large internal capacitance in the high energy PPG is created by stacking 30 single-element piezoelectric devices and electrically charging them in parallel. The internal capacitance device is also referred to as the pz stack or piezoelectric stack and is cylindrical in shape with a mass of around 30 grams.

The internal capacitance device or the piezoelectric stack of the PPG consists of piezoelectric material that requires a mechanical force to create an electric voltage. The piezoelectric materials used in this research are leaded zirconia titanates PZT 5H [5]. Figure 1 displays the piezoelectric material used in the construction of the high energy PPG. Figure 1 shows the polarity of the piezo material as marked with the black dot. This polarity is created by using a poling field of 2400 V/cm as specified by the manufacturer, APC.

Figure 1. Photograph of single piezoelectric element showing relative size. Positive polarity side of element is identified with a black dot.

One purpose of the PPG is to eliminate problems of mobility and bulkiness that occur in the case of other high power pulse generator devices. The single piezo elements act as a mechanical converter and storage of electrical energy when it is impacted by a compressive force. The piezoelectric material eliminates the use of battery power or power grids which are heavy and stationary [1]. This is made more evident in Figure 1 with the single piezo element used in the high energy PPG. Its size is smaller than the quarter on the right demonstrating the minute uniqueness of the high energy PPG. However, a large force must be supplied to compress the piezoelectric material to generate a voltage.

The mechanical force needed to compress the piezoelectric material to create a voltage can be derived from many sources. In one study, a deceleration force of a projectile containing piezoelectric material created a mechanical force [6]. However, in the research presented in this document, the mechanical force is developed from a extremely weighty steel mass. The high energy PPG is configured to operate in reverse as a force generator and is also powered by an external electrical power source. In the case of the high energy PPG, a steel mass accelerates forces to

4

compress the piezoelectric elements and generate a voltage as seen in Figure 2. Peak

forces in the order of 44 kN were obtained to compress the piezoelectric material,

thereby generating 0.7 joules of energy. Excluding the external energy storage

capacitor, high-voltage diode, and compression mass, the dimensions of the high

energy PPG is approximately 0.5″ diameter × 1.5″ length with a total mass of

approximately 470 grams.

Force

Piezoelectic
Material

+

V_{piezo}

-
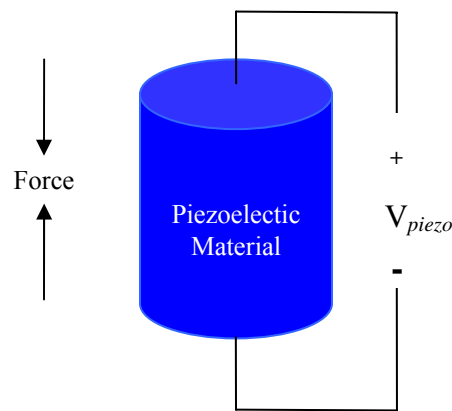
Figure 2. Illustration of compressive force needed to generate a voltage.

A computer model of the PPG system is developed and used to predict behavior.

An electromechanical model of the high energy PPG is developed in PSpice and used

to predict the performance of the high energy PPG under a variety of conditions. The

high PPG is modeled as a lumped-element mechanical system consisting of a mass,

spring, and dashpot. The PSpice simulations are compared to experimental test

results with mechanical force rise-times ranging from sub-millisecond to several

milliseconds. There is good agreement between the theoretical predictions and

experimental results. In fact, the experimental results behaved better than predicted

from the PSpice simulation. The electrical energy produced from the high energy PPG was greater than 28 kW.

The general outline of this thesis is divided into five separate sections. The first section includes the introduction, purpose, and abstract. The second section develops the theory of the high energy PPG and includes the theoretical models in PSpice. The third section illustrates the experimental arrangement used to test the high energy PPG. It goes into the testing details and general set-up and equipment used for testing procedures. The fourth section describes the results obtained at different levels to achieve the maximum power from the high energy PPG. The last section continues into the final conclusions and important characterizations of this system.

Chapter 2 Theoretical Model

The theoretical model describes the mechanical and electrical representation of the high energy PPG. It also details the computer simulation, PSpice Orcad used to develop the behavior of the high energy PPG.

2.1 Mechanical Model

In Figure 2.1, the general configuration of the high energy PPG model is depicted. Each layer of the system is marked with a different pattern. The three separate layers are the compression mass, neoprene material, and the piezoelectric material. A force is by a steel mass and is also referred to as the compression mass and the force is applied to the system. The sudden deceleration of the compression mass on the piezoelectric materials creates an output voltage. A neoprene medium is used between the piezoelectric material and the steel compress and is marked with the dots. The main purpose of the neoprene is to slow the acceleration compression of the force, thus creating a rise-time of around 5 ms. As the steel compression mass makes contact with the rubbery neoprene material, a portion of the force is absorbed, therefore limiting the total force seen by the piezoelectric material. Although, much of the neoprene can be limited to create a higher output voltage, this is one control method used to regulate the output voltage created by the piezoelectric material. The masses of the compression mass and the piezoelectric material is 11.8 kg and 0.031 kg, respectively.

A steel mass (11.8 kg) is dropped from variable height (1.015 m to 2.59 m) onto the PPG. The main purpose of the variable height is to vary the force. A neoprene

medium is used between the piezoelectric material and the compression mass. The

main purpose of the neoprene is to slow the risetime of the acceleration force on

impact with the PPG. Typically, the rise-time is approximately 5 ms. The rubbery

neoprene material also decreases the magnitude of the force. Controlling the thickness

of the neoprene layer, the size of the compression mass, and the drop height allows

one to tailor the force pulse to a wide range of magnitudes and risetimes and, thereby,

regulates the high energy PPG output voltage.
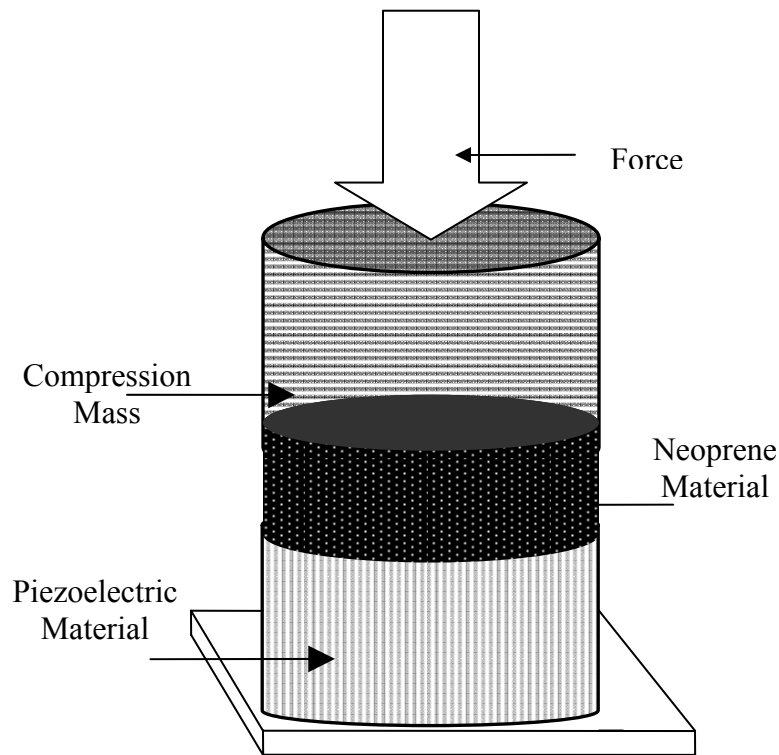
Figure 2.1. Mechanical configuration of the high energy PPG.

The high energy PPG is assumed to be a lumped element mechanical device (i.e.,

LEMD) represented by a mass, spring, and dashpot as seen in Figure 2.2. Each of

these parameters are calculated later in the section. The force is created by dropping

the steel mass onto the neoprene material. The piezoelectric material placed underneath the neoprene material and is the basis for the high energy piezoelectric pulse generator (PPG). Displacement occurs when the material is compressed together over a distance and is noted when x=0.

Figure 2.2. Mass spring model of the high energy PPG.

Parameters for the LEMD are calculated as follows:

1. Area (m^2)

   a. Compression Mass

   $$A_{compress} = \pi r_{compress}^2.$$

   b. Piezoelectric Material

   $$A_{piezo} = \pi r_{piezo}^2.$$

Area is calculated and converted to meters even though the radius is measured in centimeters. The area is also referred to as the cross sectional area and used to calculate the following constants:
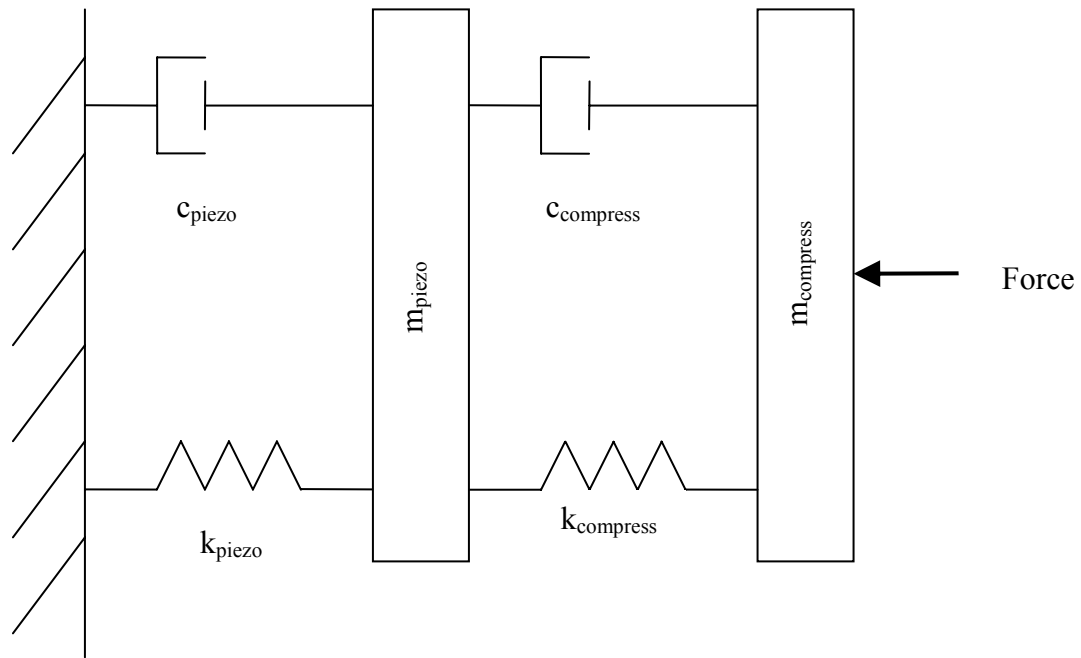
2. Spring constant (N/m):

    a. Compression Mass

$$k_{compress} = \frac{Y_{33}A_{compress}}{\ell_{compress}} \text{ [1].}$$

    b. Piezoelectric Material

$$k_{piezo} = \frac{Y_{33}A_{piezo}}{\ell_{piezo}} \text{ [1].}$$

where Y_{33} is Young's modulus (5.1 E10 N/m^2 for the APC-855 material), and ℓ is the length of the piezoelectric element and the length of the neoprene material. The length is also measured in meters.

3. Damping constant (viscous friction)

    a. Compression Mass (N·S/m)

$$c_{compress} = \frac{\sqrt{Y_{33}\rho_{compress}}}{A_{compress}} \text{ [1].}$$

    b. Piezo Material (N·S/m)

$$c_{piezo} = \frac{\sqrt{Y_{33}\rho_{piezo}}}{A_{piezo}} \text{ [1].}$$

where ρ is the mass density of the piezoelectric material and the neoprene material. Also, Y_{33} is Young's modulus (5.1 E10 N/m^2 for the APC-855 material) .

4.   Mass: the mass of the PPG plus the compression mass.

a. Mass of system

$$m_{piezo} + m_{compress} + m_{forcemass} = m_{ppg}.$$

The LEMD models the high energy PPG as long as ℓ/v_s is much less than the characteristic time of the pressure pulse, where v_s is speed of sound through the PZ material. With $v_s = 3400$ m/s and $\ell = 7.62$ E-4 (i.e., 30 mils), the characteristic time is 2.24 E-7 seconds.

In Figure 2.2, the mechanical model of the high energy PPG displays the lumped elements seen on the mechanical side. It uses a force derived from a steel mass. Then the steel compresses the masses of the neoprene material (referred with the subscript of compress) and the piezoelectric material as seen in the figure with the elements. Included in this figure are the dashpots of the piezoelectric material and the neoprene material along with the spring constants of the piezoelectric stack and the neoprene material.

It is assumed Figure 2.2 is a two degree freedom system since the system is comprised of only two main parts. Knowing the two main parts, the spring constant, system mass, and damping constant, two second order equations can be calculated to find the acceleration of the compressive mass by using the equation seen below

$$mx'' + cx' + kx = F \; [9].$$

Equation 1 takes into account the mass, velocity, spring constant, velocity, damping constant, and the displacement of the system. By using the above equation,

11

one can derive two second order equations. Equations 1 and 2 are the two second order equations and are as follows:

$$F = x_p'' m_p - x_c' c_c + x_p' (c_p + c_c) - x_c k_c + x_p (k_p + k_c) . \ (1)$$

$$F = x_c'' m_c + x_c' c_c - x_p' c_c + x_c k_c - x_p k_c . \ (2)$$

In these equations x_p'' stands for the piezo acceleration, m_{piezo} stands for the mass of the piezo material, x_p' is the velocity of the piezo material, and c_{piezo} designates the piezo damping constant, and k_{piezo} stands for the spring constant of the piezo material. For the compression side, x_c'' is the acceleration of the neoprene material, $m_{compress}$ is the mass of the neoprene material, x_c' is the velocity of the neoprene material, $c_{compress}$ is the damping constant of the neoprene material, and $k_{compress}$ is the spring constant of the neoprene material [5]. These equations were used to simulate a computer model noted later in the paper under simulation results.

2.2 Electrical Model

The electrical model of the high energy PPG can be represented as a simple RC circuit seen in Figure 2.3. The high energy PPG is connected to an external capacitor measured to be 0.1 µF to store its generated energy. The purpose of this capacitor is to hold the charge created by the piezoelectric material for 5 ms. The formula for the time constant is given

$$\tau = R_{Loss} C .$$

Where R_{loss} is the series resistance of the piezoelectric material at a given frequency. As proven in the formula, the larger the capacitance or resistance, the longer the time constant. It is due to the internal dielectric loss of the piezoelectric material. It is also defined as

$$R_{Loss} = \frac{\tan \delta}{\omega C_{piezo}}.$$

$$\omega = 2\pi f.$$

An equivalent electrical circuit of the high energy PPG is shown below in Figure 2.3. The *V stack* voltage source in series with the *C stack* capacitor is the electrical equivalent of the PPG. The *V stack* voltage source and the *C stack* capacitor represent the piezoelectric material. The piezoelectric material has a corresponding capacitance and a voltage once compressed. The diode is used to rectify the high energy PPG current. The diode has a high-voltage rating at 3 kV, while the external capacitor is manufactured by Murata Electronics, North America and has a high voltage rating of 3 kV. The capacitors are placed in a series of 3 ceramic surface-mount capacitors (GRM55DR73A104KW01L). With a PPG output voltage of 1000 volts and an energy storage capacitance of 0.1 μF, the total energy storage is given by

$$E = \frac{1}{2}CV^2.$$

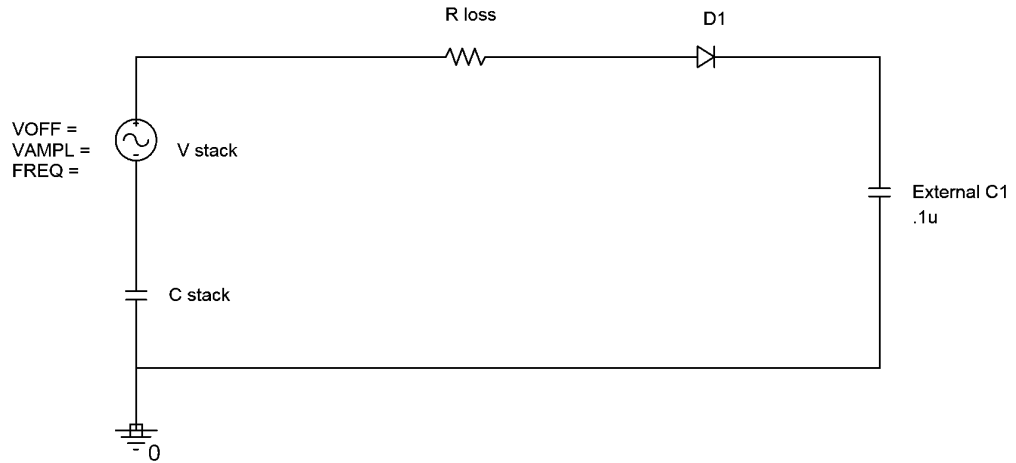Using the above equation results in approximately 50 mJ of stored energy.

Figure 2.3. Electrical model representation of the high energy PPG.

The high energy PPG has been modeled extensively. The simulation was done in PSpice circuit simulation and is detailed in the next section.

2.3 Simulation Results

The high energy PPG was modeled extensively using PSpice Orcad 10.0i version 3. The force of the system can be defined by the following differential equations. These equations were discussed in the earlier chapter.

$$F = x_p^{''} m_{piezo} - x_c^{'} c_{compress} + x_p^{'} (c_{piezo} + c_{compress}) - x_c k_{compress} + x_p (k_{piezo} + k_{compress}) \, .$$

$$F = x_c^{''} m_{compress} + x_c^{'} c_{compress} - x_p^{'} c_{compress} + x_c k_{compress} - x_p k_{compress} \, .$$

Once knowing these equations and the parameters (spring constant, damping constant, and mass), then one can solve the velocity and acceleration of the system.

14

The following equations solve for the acceleration

$$x_c'' = \frac{x_p' c_{compress} - x_c' c_{compress} + x_p k_{compress} - x_c k_{compress} + F}{m_{compress}}.$$

$$x_p'' = \frac{-x_p' (c_{ccompress} + c_{piezo}) + x_c' c_{compress} - x_p (k_{piezo} + k_{compress}) + x_c k_{compress} + F}{m_{piezo}}.$$

Both of the above equations were used to model the PSpice model as seen in Figure 2.4.

Figure 2.4 represents the computer model of the second-order equations. Outputs for the Figure 2.4 system include *v_piezo* and *x_piezo*, the velocity and acceleration of the piezoelectric stack, respectively. Additional outputs listed as *v_compress* and *x_compress* include the velocity and the acceleration for the neoprene material. This model consists of eight ABM blocks, two gain blocks, and four integrators. An important observation from this model is these outputs were each integrated to get the result. For example, *v_piezo* was integrated once to obtain the piezoelectric stack velocity, while *x_piezo* was integrated twice to obtain the piezoelectric stack velocity. The known variables used for this model are listed below under parameters. These known parameter equations are listed in the mechanical model section. The force generated is discussed on the next page.
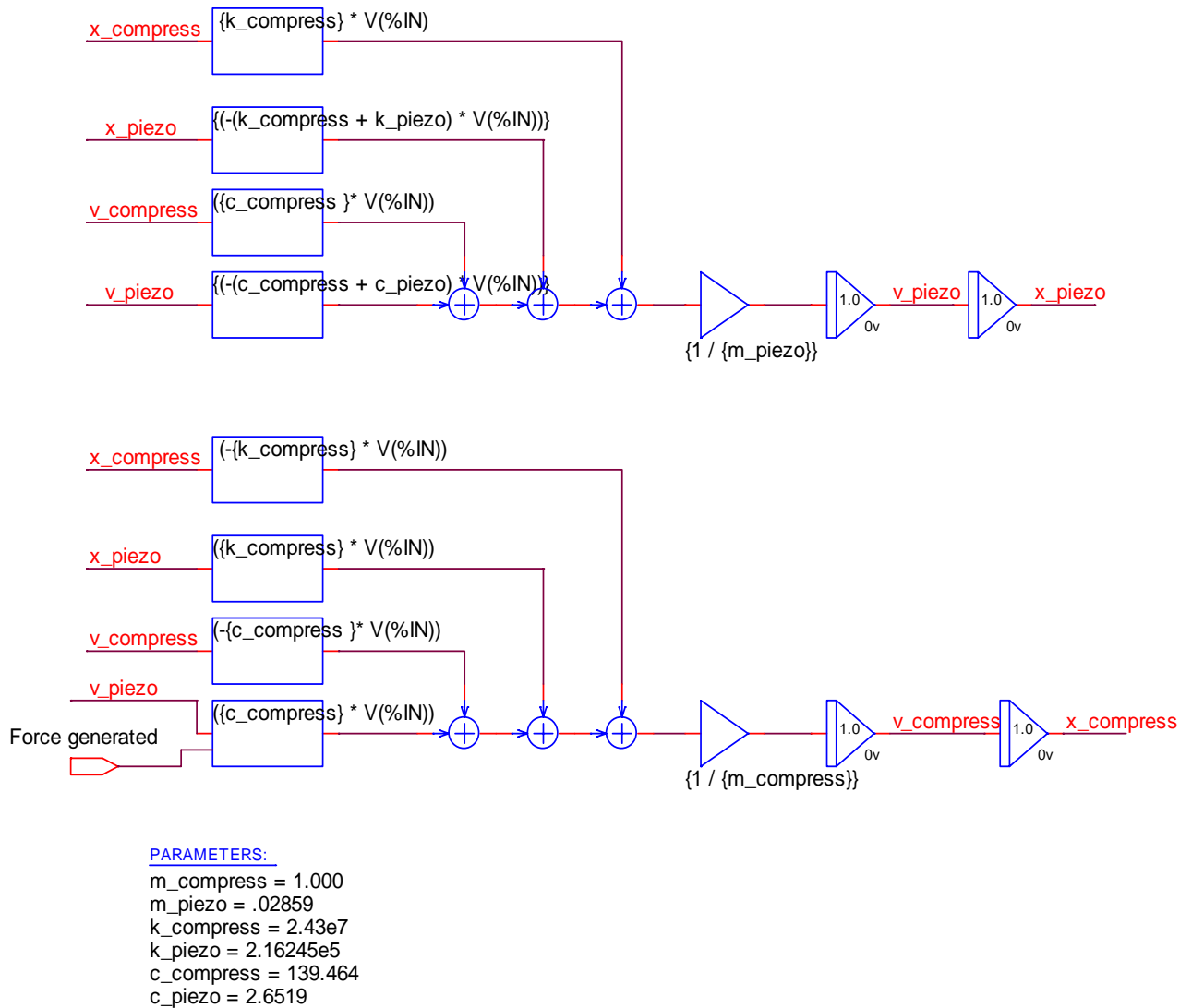
Figure 2.4. Second order model of the high energy PPG.

The generated force displayed in Figure 2.4 is calculated using PSpice in Figure 2.5. Multiplying the acceleration and the total mass give the force exerted on the piezoelectric voltage, an output of the Figure 2.5 system.

The acceleration profile is displayed in Figure 2.6. After simulating Figure 2.5, then the force was determined and then used to establish the acceleration profile in Figure 2.6. Knowing that 1kGee is equal to 9810 m/s^2 then it shows the acceleration

peaks around 6 ms. The acceleration profile is used later in determining the theoretical model data trend line.
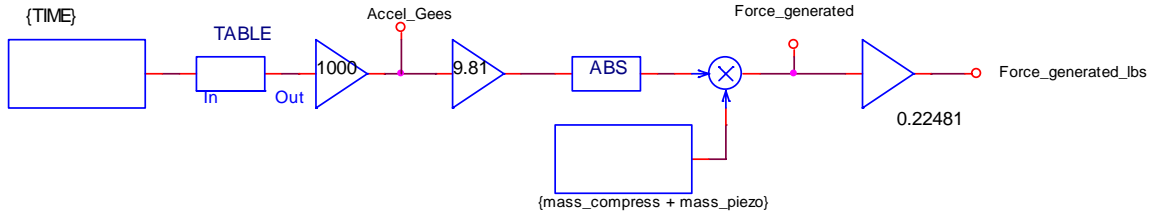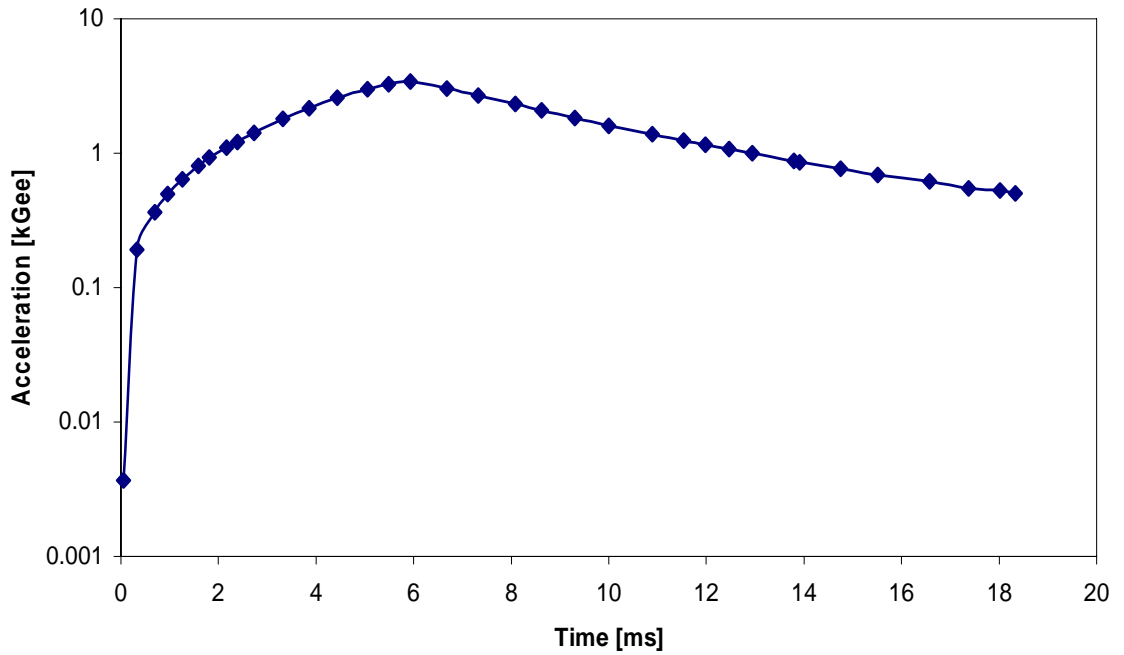

Figure 2.5. Force calculation for the PSBG.

Figure 2.6. Acceleration profile.

The product of *v_piezo* and *force_generated* are integrated to find the mechanical work of compression, *Wmech*, as shown in Figure 2.7. The piezoelectric stack voltage, *Vstack*, is also found in the Figure 2.7 system as

$$Vstack = k_{33}\sqrt{\frac{2\,Wmech}{Cstack}} \quad [1].$$

17

$$k_{33} = \sqrt{\frac{\pi \times f_{min}}{2 f_{max}} \tan \frac{\pi}{2} \frac{(f_{max} - f_{min})}{f_{max}}} \quad [2].$$

Where f_{max} is the frequency of maximum impedance and f_{min} is the frequency of minimum impedance while k_{33} is piezoelectric electromechanical coupling factor of around 0.76 according to APC data sheets and

$$C_{stack} = \frac{\varepsilon_0 \varepsilon_r A}{\ell} \quad [1].$$

Cstack is the capacitance of the piezoelectric stack. The piezoelectric stack voltage is also limited to the product of its thickness and the poling field. According to APC data sheets the value of the poling field is around 2400 V/mm for APC-855. The thickness dimension of each piezo element is approximately 0.762 mm.

$$V_{max} = V_{polingfield} \times w_{piezo} \quad [11].$$

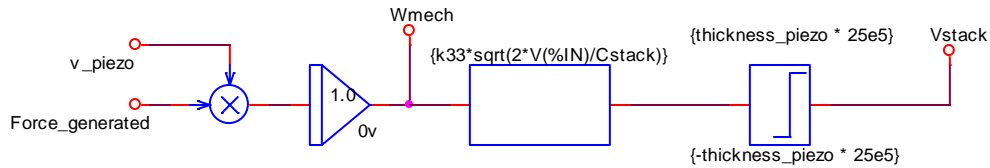So the maximum voltage for the high energy PPG was calculated with results around 1800 volts.

Figure 2.7. Calculating the PZ element voltage from the mechanical work performed in compression.

The PPG load consists of a rectifier diode and a 0.1 µF load capacitance described earlier. This load is shown in Figure 2.8. Outputs for the Figure 2.8 system include the load capacitor voltage, *Vout*, and the total stored energy, *Eout*.
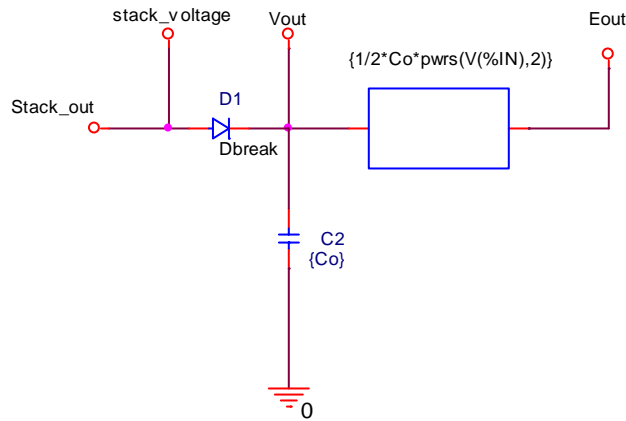
Figure 2.8. Load formed with energy storage capacitor and rectifier diode.

Each piezoelectric material is associated with a limit of temperature, voltage, and stress. The chemical composition of the material determines the limits. At elevated temperatures, piezoelectric performance decreases and the maximum safe stress level is reduced. However, the simulations operate on the assumption of room temperature (30K).

The high energy PPG is composed of PZT-5H, and other simulation calculations include the piezoelectric element compressive stress as shown in Figure 2.9. Most ceramic piezoelectric materials have a maximum stress limitation on the order of 250 MPa. Operating the high energy PPG outside of this limit may cause partial or total depolarization of the material, and a diminishing loss of piezoelectric properties [2].

The high energy PPG is used as an impact application so the PPG behaves non-linearly for pulse durations for a few milliseconds or more. When the pulse duration approaches a microsecond, the piezoelectric effect becomes linear, due to the short application time compared to the relaxation time. In the high energy case, there is a

19

short compression time and the relaxation time of time of non compression is seconds.
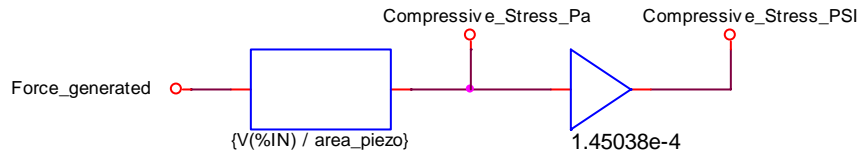
Figure 2.9. PZ compressive stress calculations.

While the piezoelectric elements are mechanically compressed in series, their electrical connection is done in parallel as shown in Figure 2.10 on the following page. As stated earlier, there are 30 total piezoelectric elements in the piezoelectric stack and is the basis for the high energy PPG. The total 30 PZ elements are referred to as the piezoelectric stack or PZ stack. The measured capacitance of each piezoelectric stack ranges from 145 nF to 154 nF. The individual piezoelectric elements also include a parallel leakage resistance 2.5 E6 Ω and a series loss resistance 12 Ω, both of which are measured quantities.
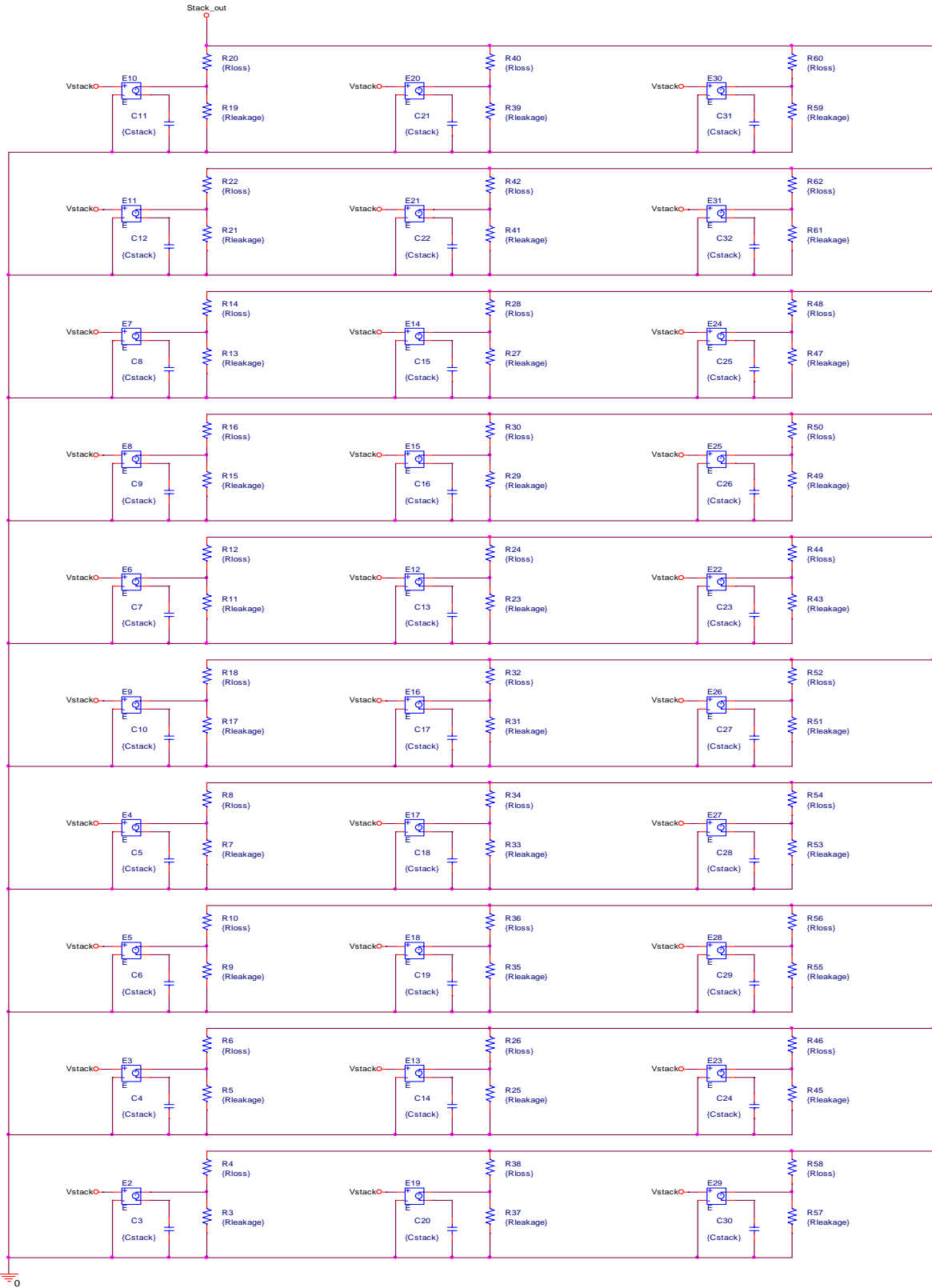
Figure 2.10. Parallel connection of 30 piezoelectric elements.

PSpice results and simulations displayed in Figure 2.11. The graph was completed in a software program, PSI plot. This software plots the voltage in volts force in newtons as seen in Figure 2.11. This data is also referred to as the theoretical model. This is in good agreement with the results discussed in the next section.

Figure 2.11. Theoretical data line based on PSpice results and simulations.

Chapter 3 Experimental Arrangement

The experimental arrangement of the high energy PPG includes a test stand, compression mass, neoprene material, piezoelectric fixture, force sensor, load/voltage divider, and the oscilloscope. Each one of these elements will be discussed below including the purpose of each component, the dimensions and material of each element. The first discussion will focus on the general overview of the system and the system connections.
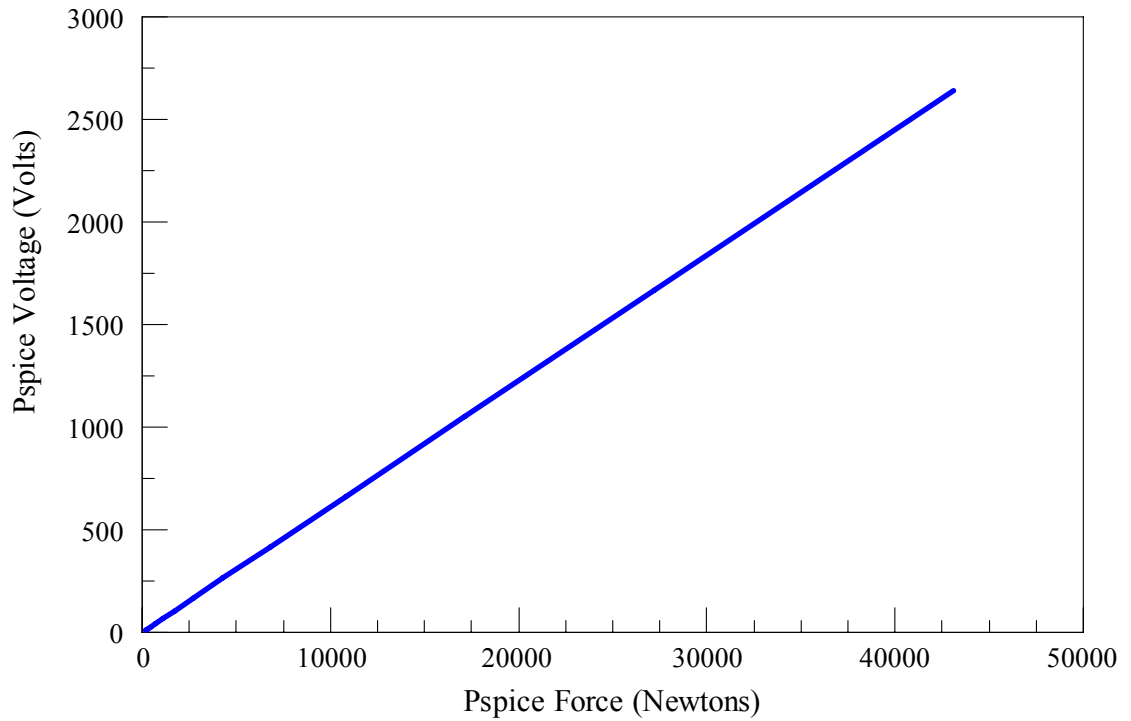
3.1 General Overview

The high energy PPG experimental arrangement connections are shown in Figure 3.1. The elements of Figure 3.1 are not to scale. As seen in the pictures, the piezoelectric stack is connected to the voltage divider and then to the oscilloscope to measure the output voltage. Both the positive and negative connection from the piezoelectric stack are connected to the voltage divider. The steel mass used to generate a force by compressing the neoprene and piezoelectric stack is not shown. The neoprene material is shown as the on top of the piezoelectric material. The force sensor located at the bottom of the picture is connected to the signal conditioner and then to the oscilloscope to measure the output force for each test. The purpose the signal conditioner is to condition the force output to exclude any noise. This will be analyzed more in depth later in this section.

23
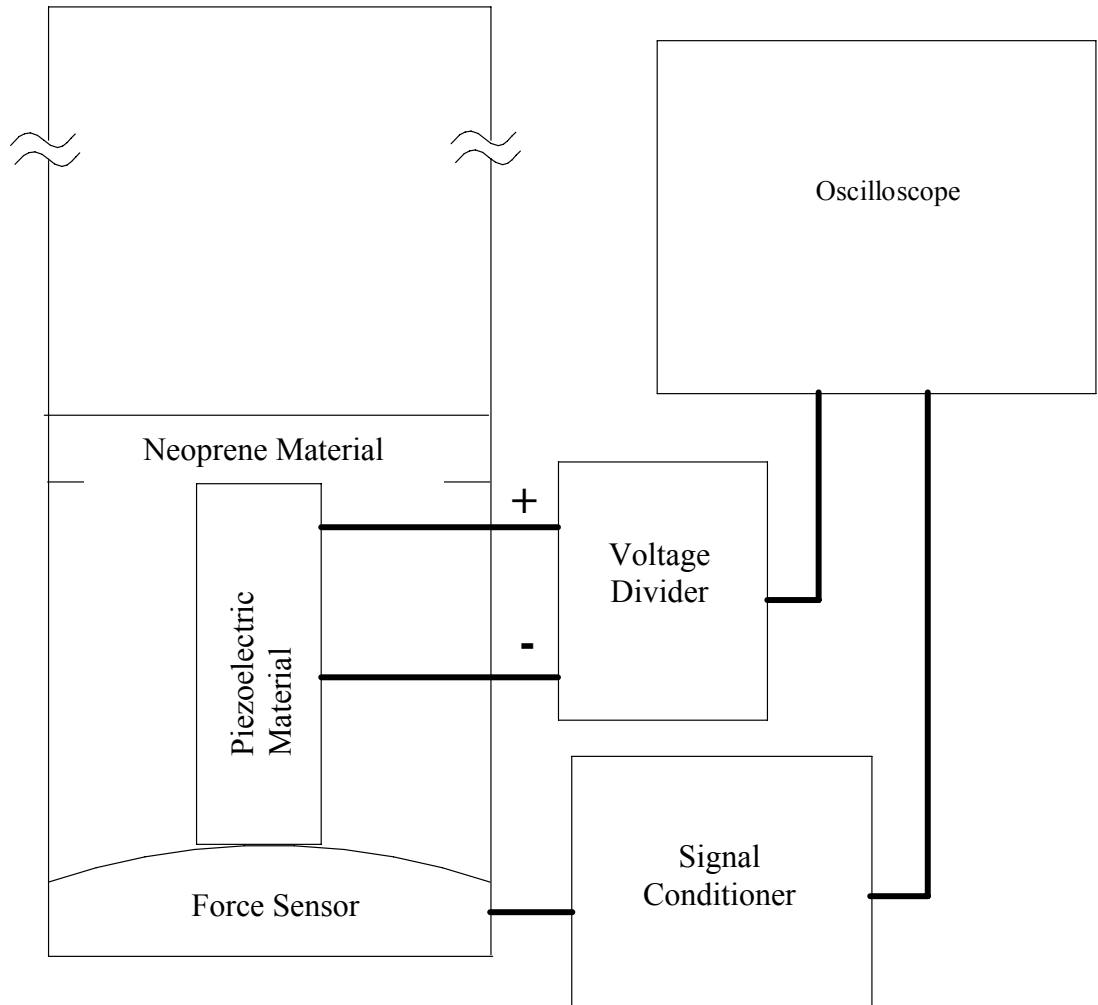
Figure 3.1. Display of connections in the experimental arrangement.

On the following page, Figure 3.2 is a more detailed drawing of the experimental

arrangement of the high energy PPG. It shows an actual picture of the system used in

the lab. A steel mass of approximately 26 kg is dropped from varying height of 1.22

m to 3.05 m onto the PPG. A neoprene medium is used between the piezoelectric

material and the compression mass. The main purpose of the neoprene is to slow the

risetime of the acceleration force on impact with the PPG. As mentioned before, the

rise-time is on the order of 5 ms. The rubbery neoprene material also decreases the

magnitude of the force. Controlling the thickness of the neoprene material, the size of the compression mass, and the drop height allows one to tailor the force pulse to a wide range of magnitudes and risetimes and, thereby, regulate the high energy PPG output voltage.

Figure 3.2. Experimental arrangement of the high energy PPG.

3.2 Test Stand
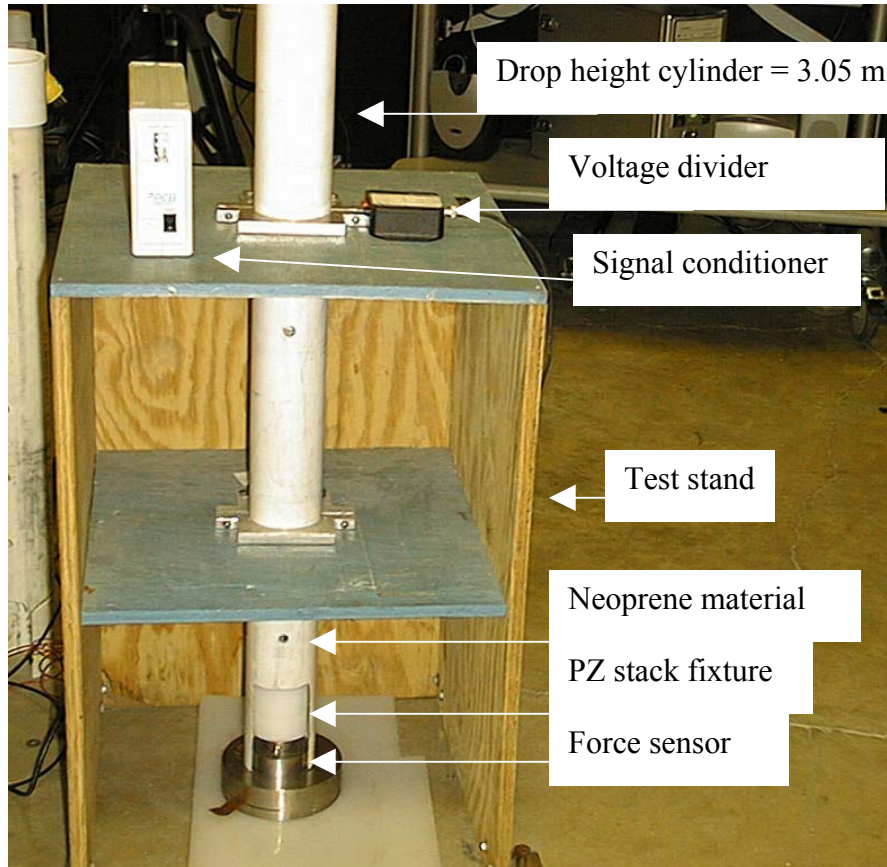
The next element to be discussed is the test stand. The test stand consists of a PVC pipe to guide the compression mass. The cylinder is held upright in a wooden fixture. Figure 3.3 roughly displays the outline of the combined elements in the test stand. It consists of a drop height that is a PVC tube with a total length of 3.05 m. The cylinder has 12.7 mm holes drilled into the pipe every 0.13 m on one side. The main purpose for the drilling of the holes is to release pressure when the steel mass is dropped down the tube. The steel mass is dropped from varying heights from 1.219 m to 3.048 m. The bottom of the drop height is drilled out to create a space for the piezoelectric stack fixture and the force sensor. This makes testing easier and quicker along with more accurate results.

The stability component of the testing stand consists of a wooden fixture with a height of 0.79 m and length of 0.51 m. The purpose wooden fixture is to support the PVC pipe, to assure it stays in one direction. This creates a more reliable experimental arrangement. Both elements of the test stand are displayed in Figure 3.3 The next component to be discussed is the compression mass that is placed within the PVC pipe.
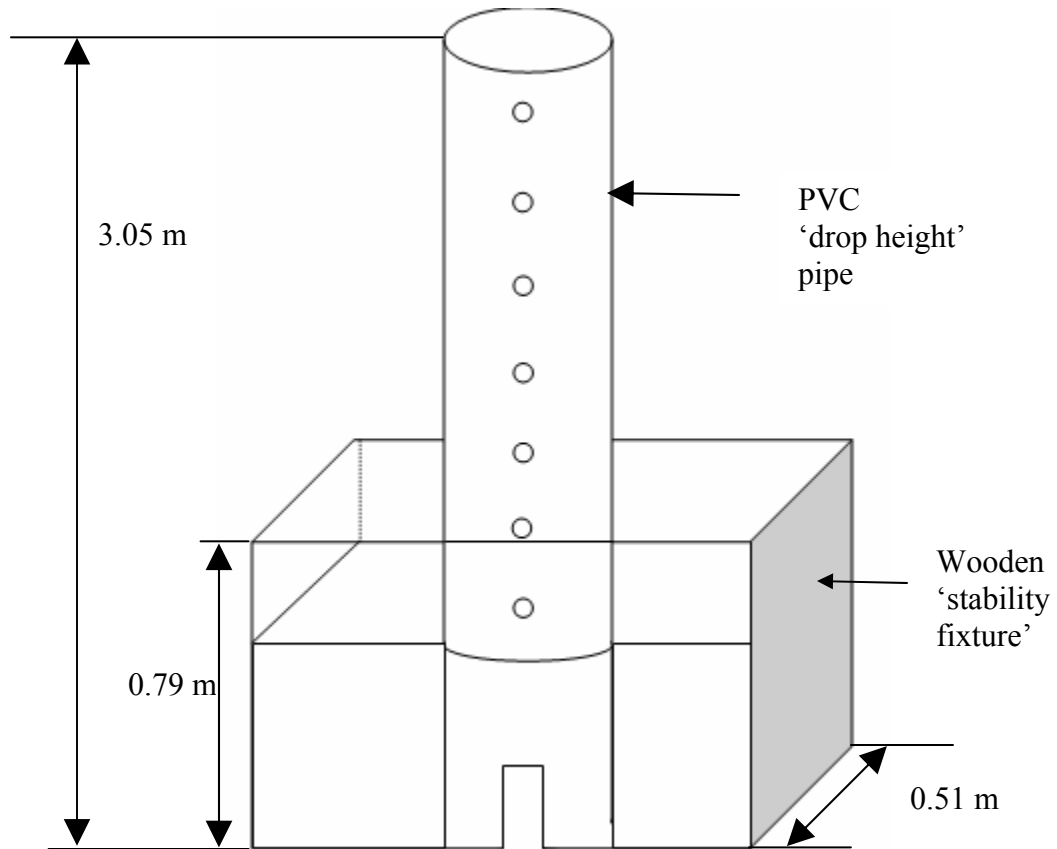
Figure 3.3. Display of drop height and stability fixture.

3.3 Compression Mass

The steel mass or the compression mass is placed inside of the drop height tube to compress the neoprene, piezoelectric stack fixture, and force sensor. It is dropped from varying heights in the drop height cylinder, the purpose of the variance is to control the magnitude of the force. The compression mass is composed of steel with a rounded tip and a weight around 11.79 kg. Figure 3.4 shows the length of the compression mass as 30.5 cm with a diameter of 7.54 cm, the ruler to the side is measured in inches to display the relative size. The next element of the experimental arrangement is the neoprene material.

Figure 3.4. Picture of compression mass.

3.4. Neoprene Material

Figure 3.5 displays a photograph of the neoprene disc material used in the high energy PPG experimental arrangement. The total neoprene material is compromised of 2-6 neoprene discs depending on the desired force on each test. By increasing or decreasing the thickness of the neoprene, the force can be increased or decreased. For example, on low force tests, 6 neoprene discs are used or a total thickness of 7.62 cm, resulting in approximately 6.67 kN of force.

Each neoprene disk is approximately 1.27 cm thick with a diameter of 7.54 cm and a weight of 68.55 g. As discussed earlier, the basic purpose of the neoprene material is to slow the risetime of the force to around 5 ms and to limit the amount of force on the rest of the high energy PPG system. The neoprene is placed on top of the piezoelectric stack fixture inside the PVC pipe. The neoprene material is the first material to be compressed by the steel compression mass. This was seen in earlier in Figure 3.1. The next element of the high energy PPG system is the piezoelectric stack fixture.
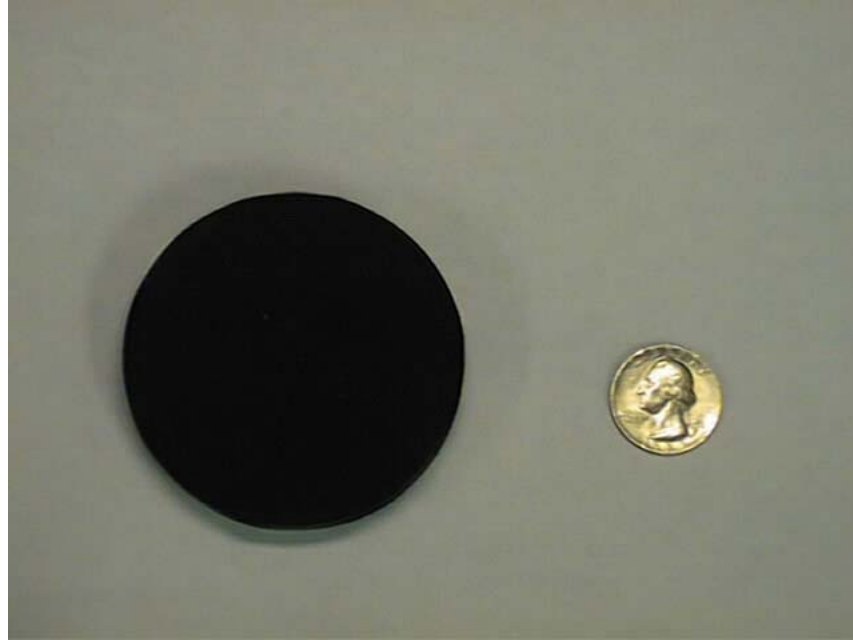
Figure 3.5. Photograph of neoprene medium showing relative size.

3.5 PZ Stack Fixture

Figure 3.6 displays a photograph of the piezoelectric stack or PZ stack element. As described in the previous section, the piezoelectric stack consists of 30 different piezoelectric elements connected in parallel. The piezoelectric elements are made of a leaded zirconia titanate PZT 5H. The elements are stacked with alternating polarity and uses copper foils between the piezoelectric elements to maintain the electrical connection. The ends of the piezoelectric disc elements are also metallized with a small amount of silver. The piezoelectric elements are bonded together with nonconductive epoxy to form the PZ stack. Leads are soldered to the copper foils to make the external connections. It is assembled into a generator or stack by the manufacturer, American Piezo Corporation (part APC-855). The dimensions of each

prototype stack have a 1.27 cm diameter with a total height of approximately 2.52 cm. Each PZ stack has a total (nominal) stack capacitance of 0.15 µF.
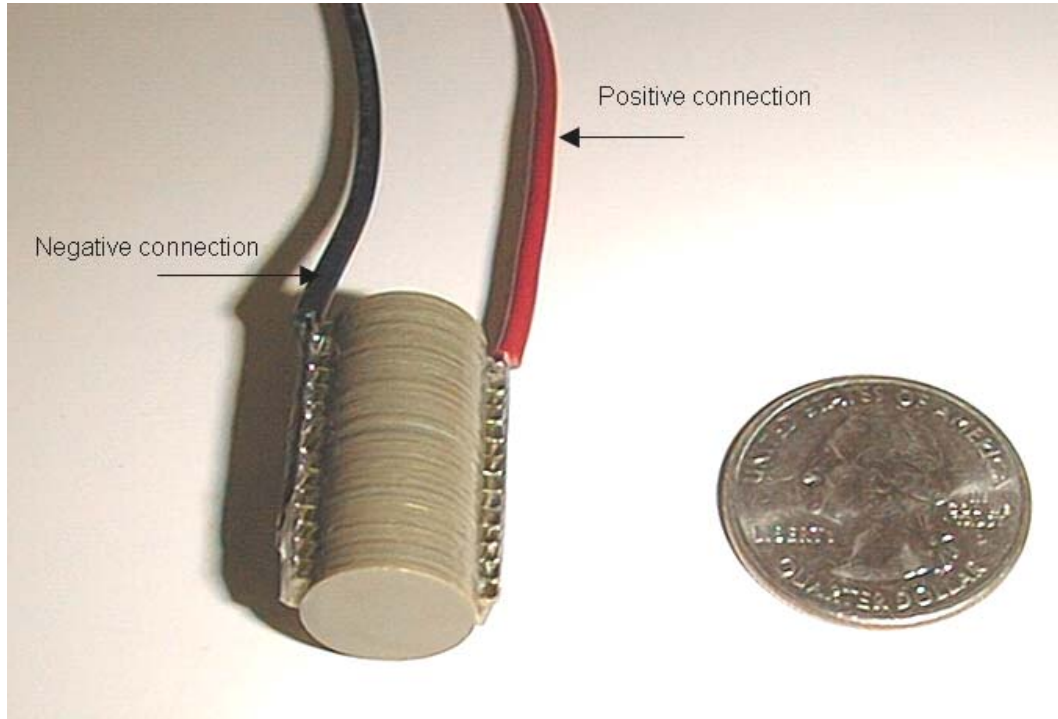
Figure 3.6. Photograph PZ stack showing relative size.

The PZ stack fixture consists of two main separate parts. The first is seen on the left in Figure 3.7 it is referred to as the threaded extenstion. It uses two bolts with a housing to secure the piezoelectric stack. The stack is placed between both bolts. Testing the individual piezoelectric stacks or generators consisted of tightening a 5/8 inch fixture bolts to approximately 5 in-oz torque (as measured by a torque watch). The second part of the PZ fixture consists of a lexan housing as seen on the right of Figure 3.7. Both components are labeled above the respective element. The purpose of the lexan housing is to maintain that the force is applied to the PZ stack. Figure 3.7

shows the separate parts of the PZ stack fixture. The arrows display the threaded extension component being placed inside of the lexan housing component. Figure 3.8 shows both the combination of both components that are the structure of the PZ fixture. Once again, the ruler on the left is in inches to show the relative size of the element. The frame of the PZ fixture has a total height of 16.51 cm with a diameter of 7.54 cm and a total weight of 0.725 kg. The PZ fixture structure is placed under the neoprene material within the drop height cylinder. Under the PZ fixture structure is the force sensor. The force sensor is discussed in the next section.
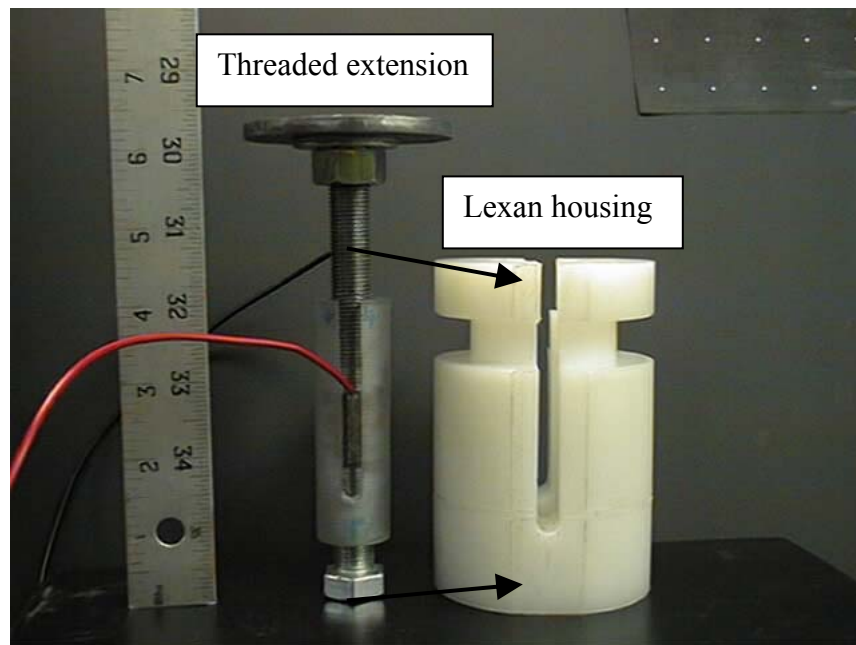
Figure 3.7. Different parts of the PZ stack fixture structure.
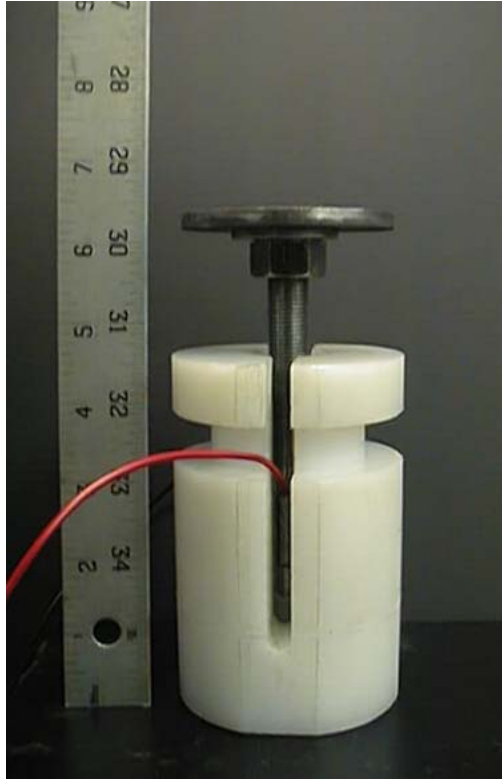
Figure 3.8. Complete PZ stack fixture.

3.6 Force Sensor

The PCB Model 200C20 force sensor and PCB Model 482A21 signal conditioner are used to measure the force and are seen in Figure 3.9 and Figure 3.10, respectively. The force sensor has a total height of 5.08 cm with a diameter of 3.30 cm and a weight of 1.05 kg. The force sensor is placed under the PZ stack fixture, inside of the drop height cylinder at the bottom. In Figure 3.9, a piece of kapton tape is placed on top of the force sensor. The tape reduces noise in the force readings. The force sensor is connected to the signal conditioner through a red coaxial cable. The signal conditioner is then connected to the oscilloscope as seen earlier in this section. The main purpose of the signal conditioner is to condition the force reading on the

oscilloscope. The signal conditioner has a total height of 15.24 cm and a total length of 25.4 cm. The weight of the signal conditioner is 0.82 kg. The next component of the high energy PPG experimental arrangement is the load/ voltage divider.
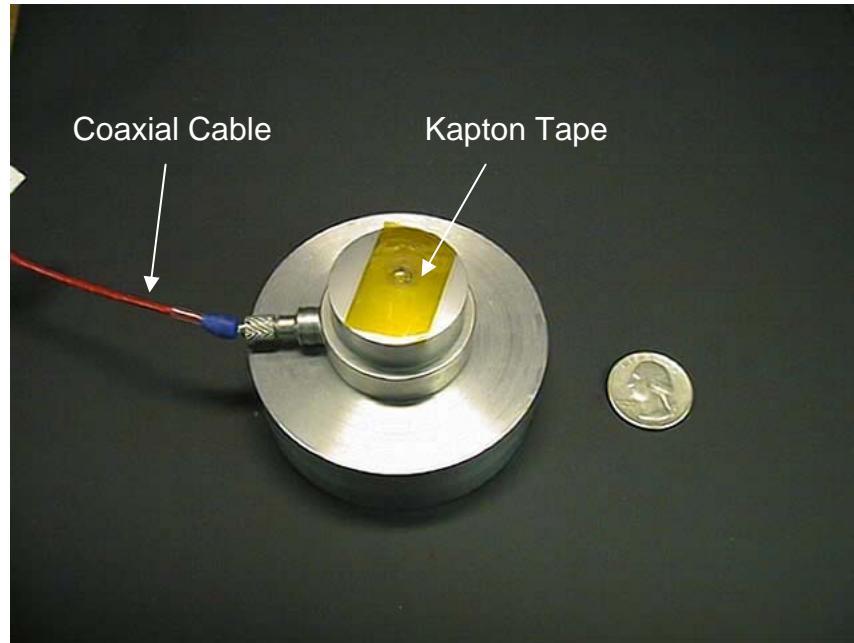
Figure 3.9. Force Sensor – PCB Model 200C20.

Figure 3.10. Signal Conditioner – PCB Model 482A21.

3.7 Voltage Divider

The PZ stack connections displayed in Figure 3.6 are used as inputs in the load/ voltage divider seen in Figure 3.11. The size of the box is 10.16 cm x 10.16 cm and weighs approximately 133.6 g. The box uses a positive and negative input connection as seen from the PZ stack in Figure 3.6. The grounding switch is used to short the PZ stack fixture in between test runs. This is crucial since voltage can build up on the individual PZ elements. The output voltage is measured with a high-impedance (100 GΩ) voltage divider (10,000:1) and recorded. This is displayed with the output to the oscilloscope connector.

The schematic of the voltage divider is shown in Figure 3.12. As mentioned earlier, it uses a high impedance (100 GΩ) voltage divider (10,000:1). Since one of the main purposes of the high energy PPG is to create over 1 kV, the voltage divider was created so the voltage does not exceed the ratings on the oscilloscope. The next element of the high energy PPG is the oscilloscope.
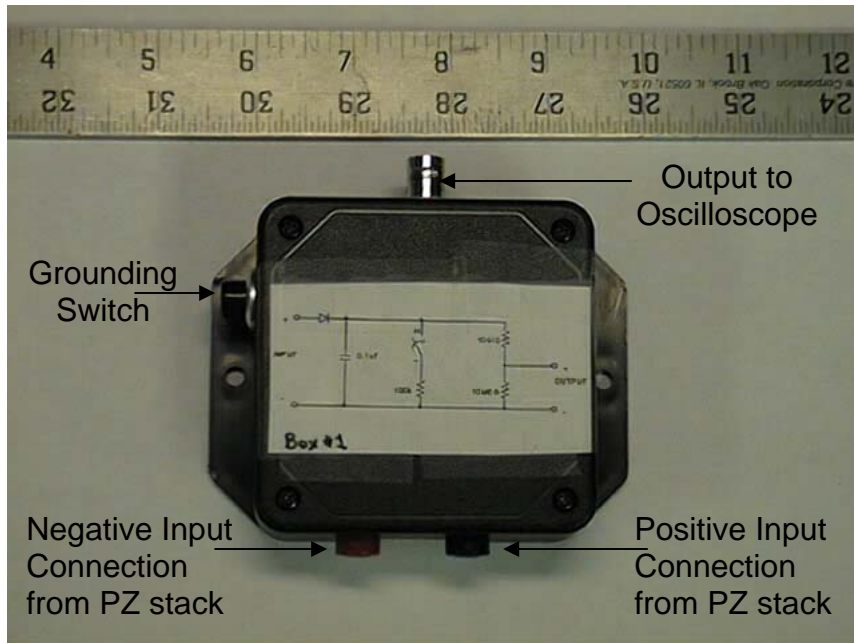
Figure 3.11. Photograph of voltage divider box.
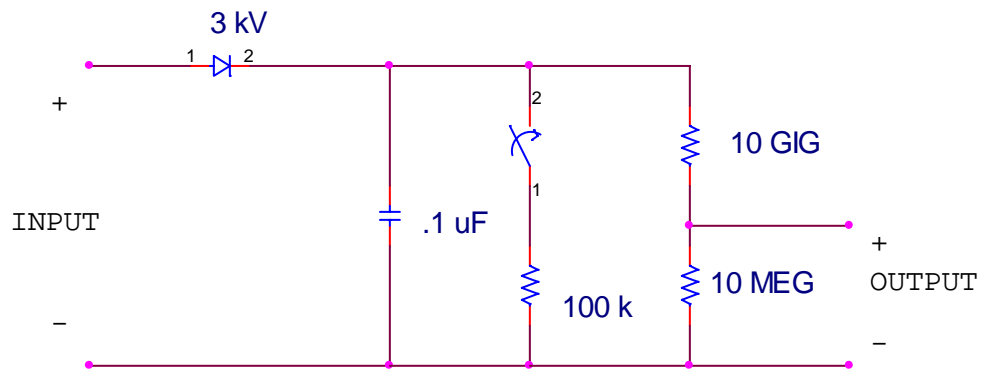
Figure 3.12. Load schematic of voltage divider.

3.8 Oscilloscope

Figure 3.13 is a photograph of a workbench oscilloscope used in the high energy PPG experimental arrangement. The oscilloscope is a Agilent Technologies model DSO6104A. This scope was used to measure the output force and output voltage of the high energy PPG. One huge benefit of using this digital scope is its ability to transfer data to a computer via the internet. So now that the experimental arrangement has been discussed, the next topic covered is the results.
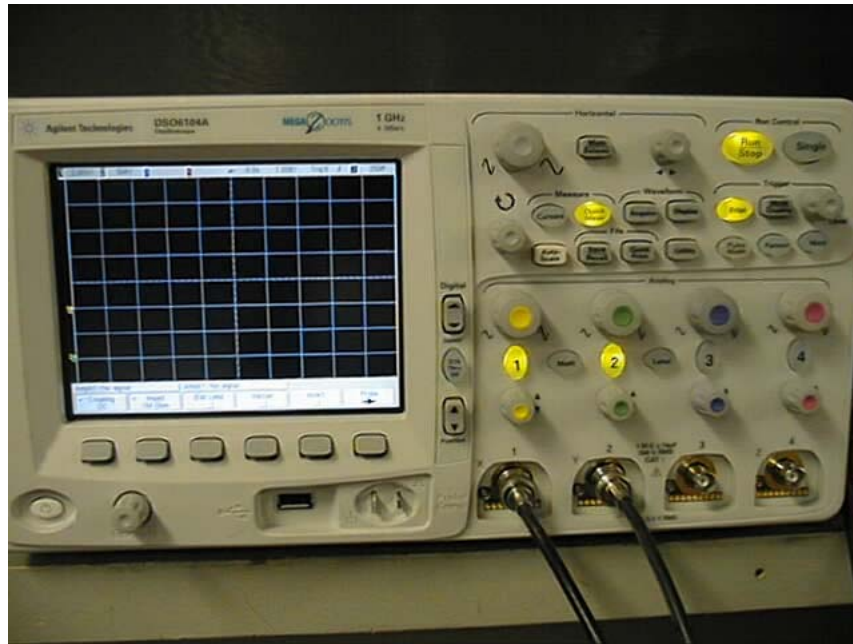
Figure 3.13. Photograph of Agilent Scope Model DSO6104A

Chapter 4 Results

The high energy PPG performed well above the theoretical limit as discussed in the Chapter 2 computer simulations. There were two prototypes tested, however, the 2nd prototype is the main focus of the high energy PPG. The results are listed into five separate categories: first prototype, low force, intermediate force, high force, and maximum voltage. Each category went through the same testing procedures as described in Chapter 3, the only differences were in the drop height and the thickness of the neoprene medium. This variance created a variance in force exerted on each piezoelectric stack. Each of the categories are described in the sections below. The first prototype is briefly discussed below.

4.1. First Prototype Overview

The first prototype consists of the same piezoelectric elements and dimensions as discussed previously in Chapter 3. The only difference is the first prototype uses foil leads for a positive and negative connection instead of soldered wires for connections. Figure 4.1 is a photograph of the first prototype assembled in its test fixture. That figure illustrates the foil leads that form the positive and negative connections to the individual piezoelectric elements and shows the test fixture used to contain the piezoelectric elements. Externally, the piezoelectric elements are connected in parallel with to form a 0.15 µF capacitance.
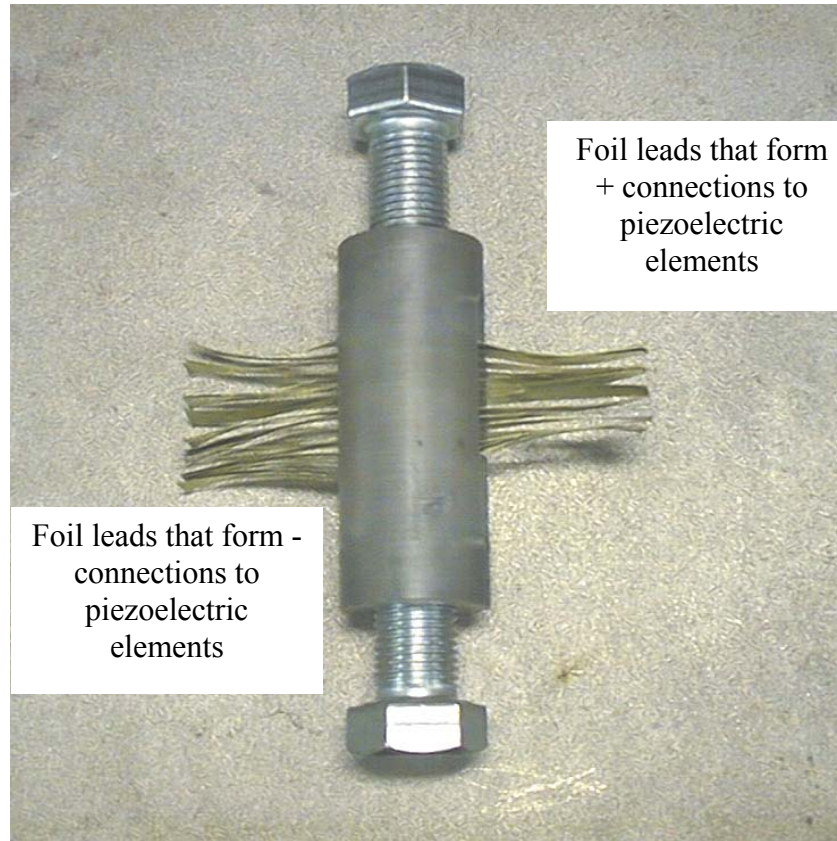
Figure 4.1. Photograph of first prototype testing PZ fixture.

Figure 4.2 shows the typical output voltage from the first prototype. The first prototype tests achieved an average output voltage of 1.2 kV, performing better than the expected 1 kV. The results were taken over a 10 second period. Much noise was noted at the beginning of this test and was attributed to static electricity created in the drop height cylinder by the compression mass. The power output on this test was approximately 15 kilowatts. The compression force measured for this test was around 18 kN.
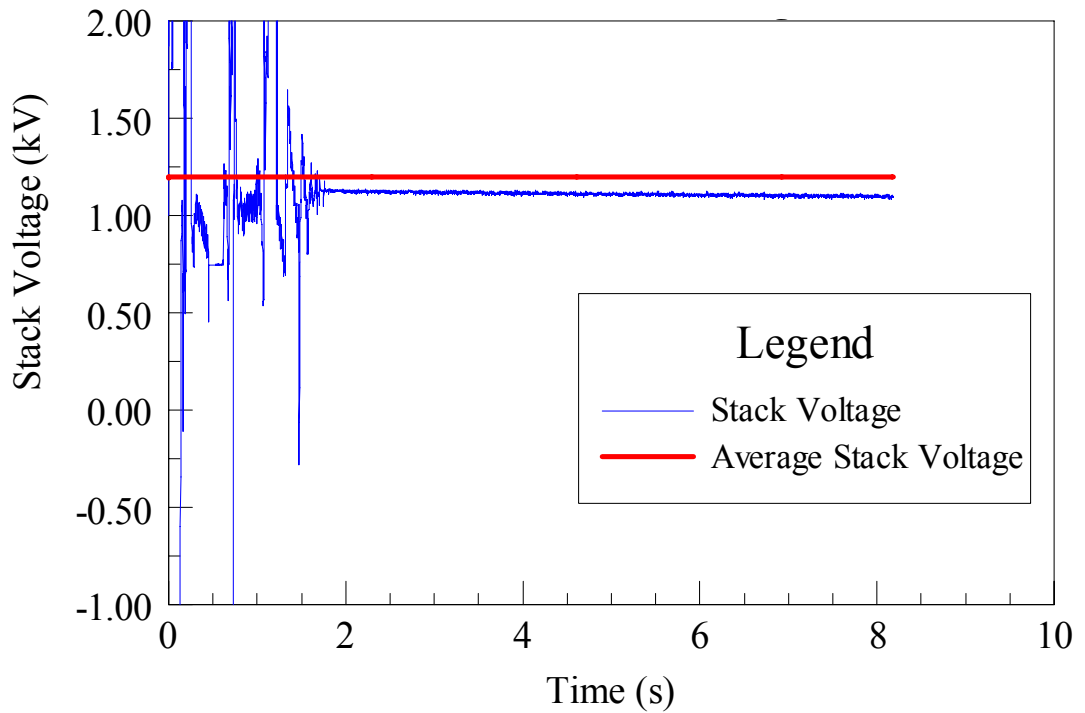
Figure 4.2. Typical measured output voltage for first prototype.

Figure 4.3 is a typical force measurement of the first prototype. The risetime is 4.5 ms. The peak force is obtained from the force sensor voltage with the calibration factor given by

$$Force_{peak} = \frac{Voltage_{peak}}{0.25} \times 4.45 . \text{ [N]}$$

Using the above calibration factor, the total force in the Figure 4.3 data is approximately 18 kilonewtons (kN). It is noted that forces as high as 89 kN can be produced with the compression mass when the neoprene is not used in the testing arrangement. Force risetimes under these conditions will be on the order of 1 μs. Use of the neoprene material reduces the peak force and slows the risetime to that shown in Figure 4.3. The risetime in Figure 4.3 is around 4.5 ms.
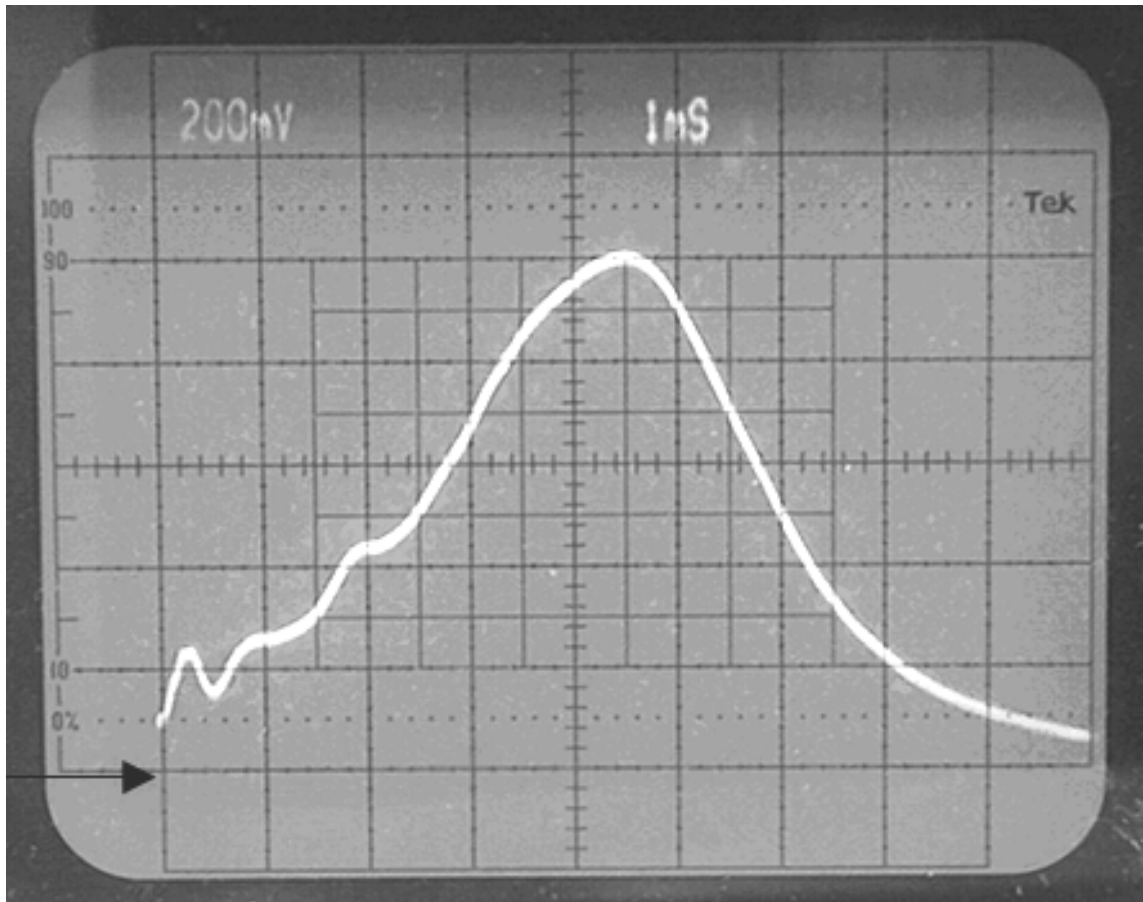
Figure 4.3. Photograph of force measurement (arrow indicates reference point).

Table 4.1 lists the output voltage from the three first prototype generators. All three generators produced the required 1000 V output for 10 s period when loaded with 18 kN of force. The highest voltage produced in testing occurred with S/N #3 on its first test where it reached 1200 volts. The compression force for this test was around 19 kN. Although it is required for a piezoelectric pulse generator to produce one output pulse, testing occurred until the piezoelectric element became chipped or cracked or until the output voltage was zero. It is noted that all three generators were broken during testing, typically on the fifth or sixth test.

The test data of Table 4.1 also show the first test runs to have the highest output voltage. All subsequent tests had lower output voltage, the only exception noted was S/N 2 which is an operator error for the first test. The results in Table 4.1 are very similar to the results seen previously Chapter 2, proving there is good agreement between the theoretical predictions and experimental results. However, the focus of the high energy piezoelectric pulse generator is on the assembled PZ stacks. Results for the low force category are detailed in the next section.

Table 4.1. Summary of first prototype experimental results.

First Prototype		
Experiment	**$V_{average}$ [V]**	**$Force_{peak}$ [kN]**
S/N #1:		
Test 1	1180	17.79
Test 2	1180	17.79
Test 3	640	16.01
Test 4	957	16.90
Test 5	692	19.57
Test 6	Broken generator	
S/N #2:		
Test 1	260	17.79
Test 2	1110	18.68
Test 3	844	19.12
Test 4	726	17.79
Test 5	Broken generator	
S/N #3:		
Test 1	1200	19.12
Test 2	1130	18.68
Test 3	1090	17.79
Test 4	1030	18.68
Test 5	652	22.24
Test 6	Broken generator	

4.2. Low Force Results

The first test sequence discussed is the low force generator. The testing is the same as described in Chapter 3. The high energy also utilizes the assembled PZ stacks discussed in the PZ fixture in Chapter 3. The low force category of test results had a lower force exerted on the high energy PPG. The force is lowered by increasing the amount of neoprene material and decreasing the height from which the compression mass is dropped. One reason for the lower force tests is to characterize the voltage from the high energy PPG. This test can distinguish the output voltages at a given force.

In the low force tests, nearly 10.16 cm of neoprene material is used to compress. The height from which the mass was dropped was only 1.106 m. Figure 4.4 below shows the decrease in force measured by the sensor. Observing Figure 4.4 and using the following equation, the total force in newtons can be calculated.

$$Force_{peak} = \frac{Voltage_{peak}}{0.25} \times 4.45 . \ [N]$$

As seen in the above equation and in Figure 4.4, approximately 7 kN force was applied with a 5 ms risetime.
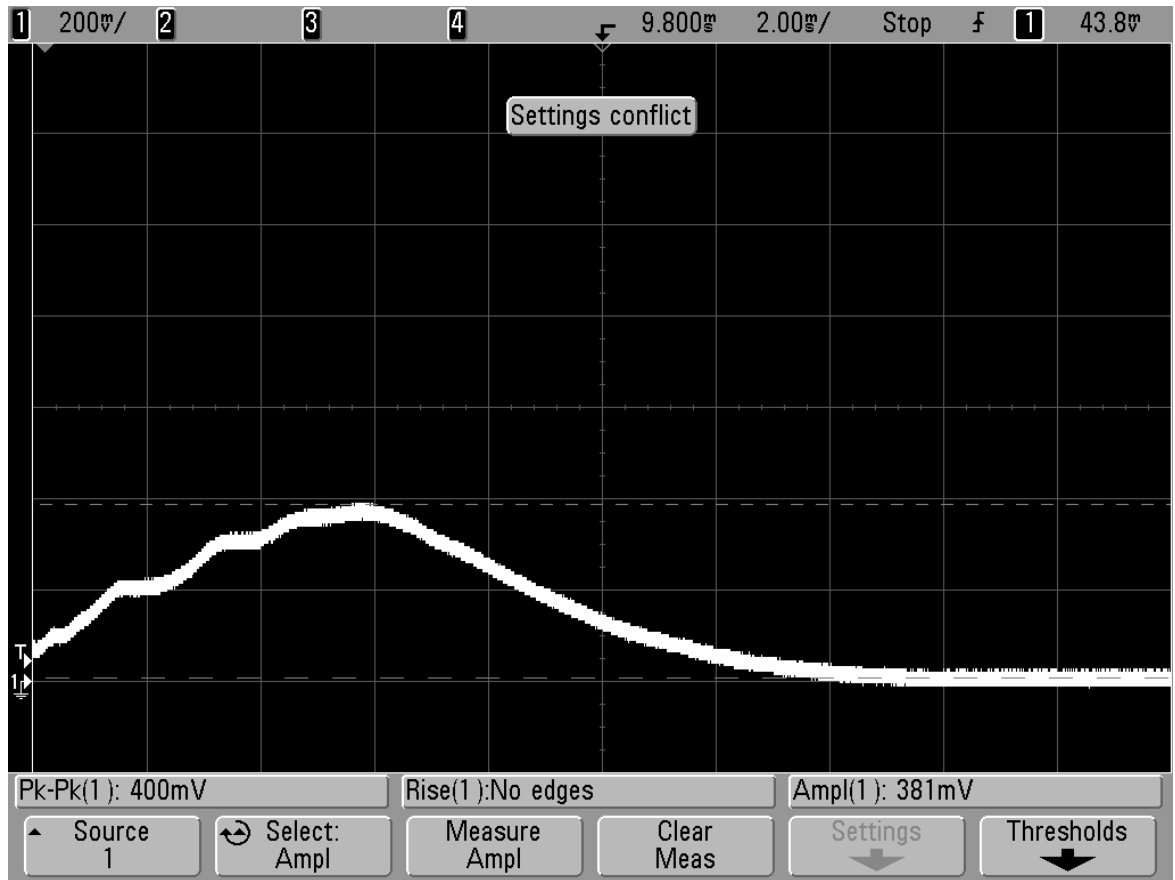
Figure 4.4. Typical force measurement for the low force category.

Figure 4.5 displays the typical output voltage on the low force category for a 10 second period. The voltage was approximately 700 volts with a corresponding 7.12 kN compressive force. Noise was noted during testing. The noise is attributed to the PVC pipe creating an electrostatic charge on the piezoelectric elements.
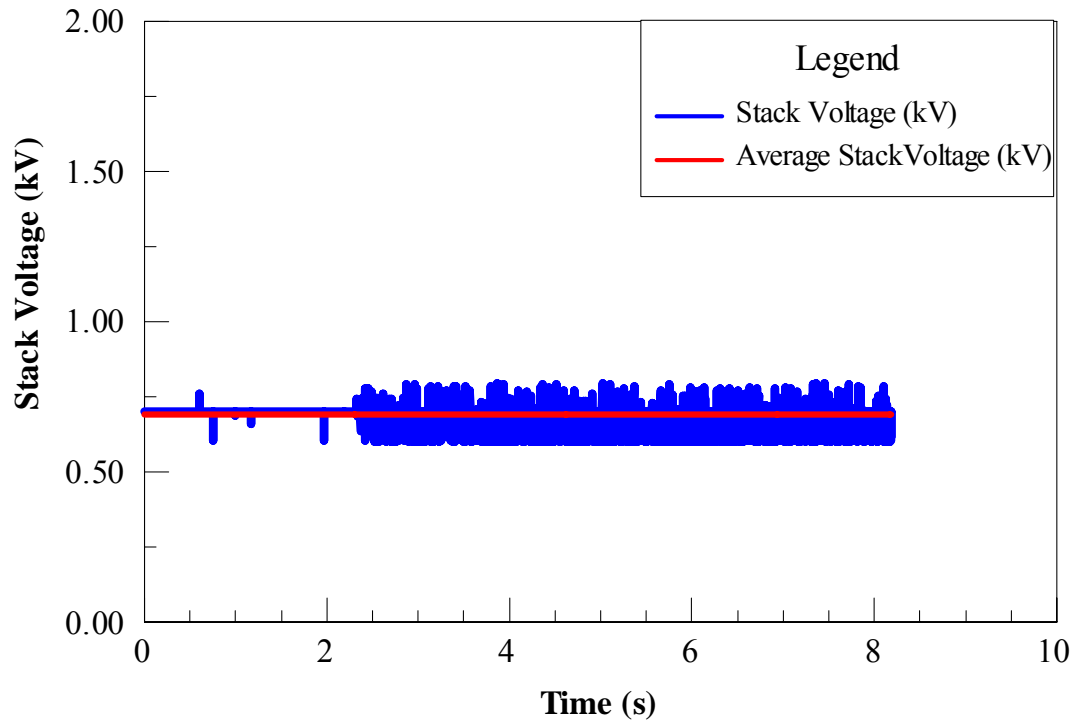
Figure 4.5. Typical voltage measurement for the low force category.

The complete results from each low force test runs are listed in Table 4.2. Each test set received around 6.67 kN to 8.00 kN of force and obtained between 475 to 700 volts. The only exception would be S/N 11 where an operator error occurred causing it to receive over 9.00 kN of force. Once again, voltage decreased between each test. An interesting observation made during this test sequence was an increase in generator capacitance and dissipation factor. Capacitance and dissipation measurements were made before any testing and once again after testing ceased. The increase in capacitance was unexpected. However, non-conductive epoxy was used by the manufacturer, APC, to bond the piezoelectric elements together. Therefore, an

air gap capacitance was formed between each piezoelectric element and the foil used

to connect the elements together.

Table 4.2. Summary of the low force experimental results.

	Experiments	$V_{average}$ (Volts)	Force$_{peak}$ (kN)	Capacitance (nF) / Dissipation Factor
Low Force*				
S/N 11:	Test 1	800	9.00	147.2 / 0.010
	Test 2	550	7.90	
	Test 3	500	7.12	
	Test 4	500	8.00	163 / 0.016
S/N 12:	Test 1	700	7.12	153.7 / 0.012
	Test 2	550	7.22	
	Test 3	475	7.22	
	Test 4	475	7.67	167.3 / 0.018
S/N 13:	Test 1	700	7.22	151.2 / 0.012
	Test 2	600	7.67	
	Test 3	600	7.46	
	Test 4	600	7.12	167 / 0.017
S/N 14:	Test 1	700	7.22	149.8 / 0.013
	Test 2	550	6.78	
	Test 3	575	7.56	
	Test 4	550	7.12	165.7 / 0.017
S/N 15:	Test 1	600	7.90	150.6 / 0.011
	Test 2	550	7.23	
	Test 3	550	7.23	
	Test 4	525	7.06	164.7 / 0.016
S/N 16:	Test 1	600	7.12	148.4 / 0.010
	Test 2	550	7.12	
	Test 3	550	7.56	
	Test 4	550	7.23	163.7 / 0.016

* Low force group was taken to an approximate height of 1.016 m and used 10.16 cm of neoprene.

Figure 4.6 is a plot of all the tests performed at the low force category. An

important observation is that the first test performed the highest. The second, third,

and fourth test performed similarly. This is repeatability is seen in Figure 4.6 for each

individual test set. Once again, S/N 11 experienced over 9 kN of force due to operator error and is seen at the top of the figure. Test 1 shown with the circle symbol performed the highest at 700 volts and approximately 7 -8 kN of force. However, all of the tests performed above the theoretical model. The reason for this is the electromechanical coupling factor is much higher than specified in the manufacturer's data sheets. The next category of results is the intermediate force grouping.
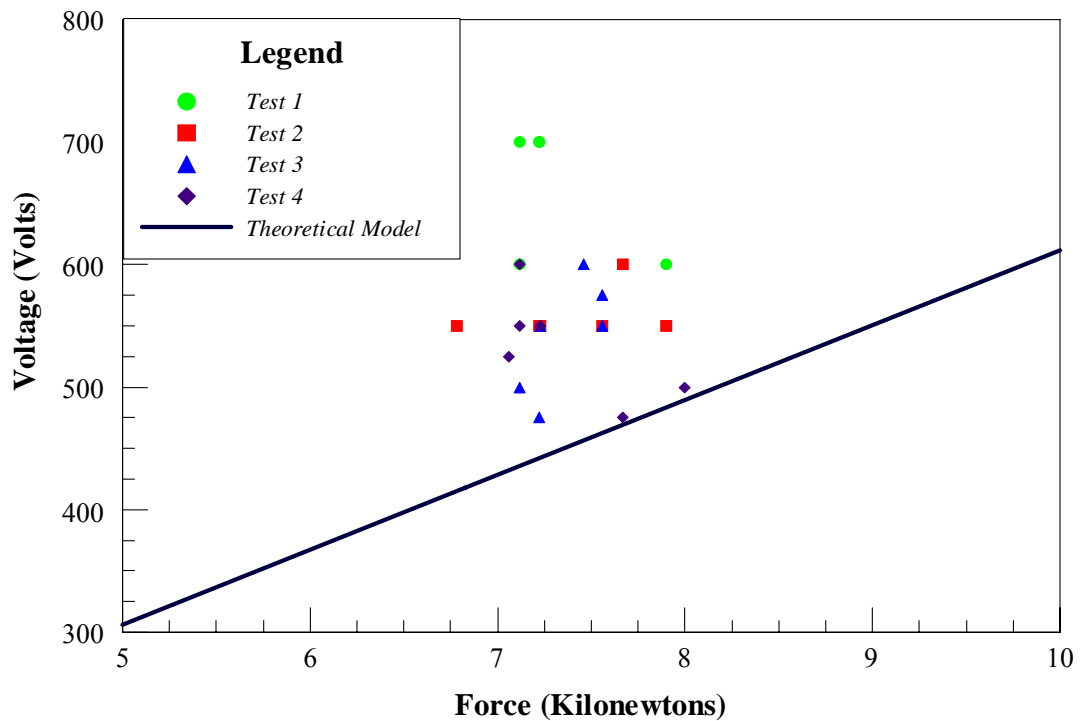

Figure 4.6. Low Force Results.

4.3 Intermediate Force Results

The intermediate force category is tested in the same manner as the low force. The intermediate category used 8.89 cm of neoprene material while the drop height is 1.37 m. This produced a force between 8.90 kN to 11.57 kN. Figure 4.7 shows the typical force profile for the medium force tests with approximately 11.12 kN of force and a risetime of 4.8 ms. Risetime is measured between 0 – 100% of the peak force. Figure 4.8 is the typical output voltage from each medium force test. The average stack voltage is 1050 volts with an average 11.12 kN of force. The force decreased by 50% from 22.24 kN to 11.12 kN and yet the intermediate force category had each test perform over 1000 volts on the first test.
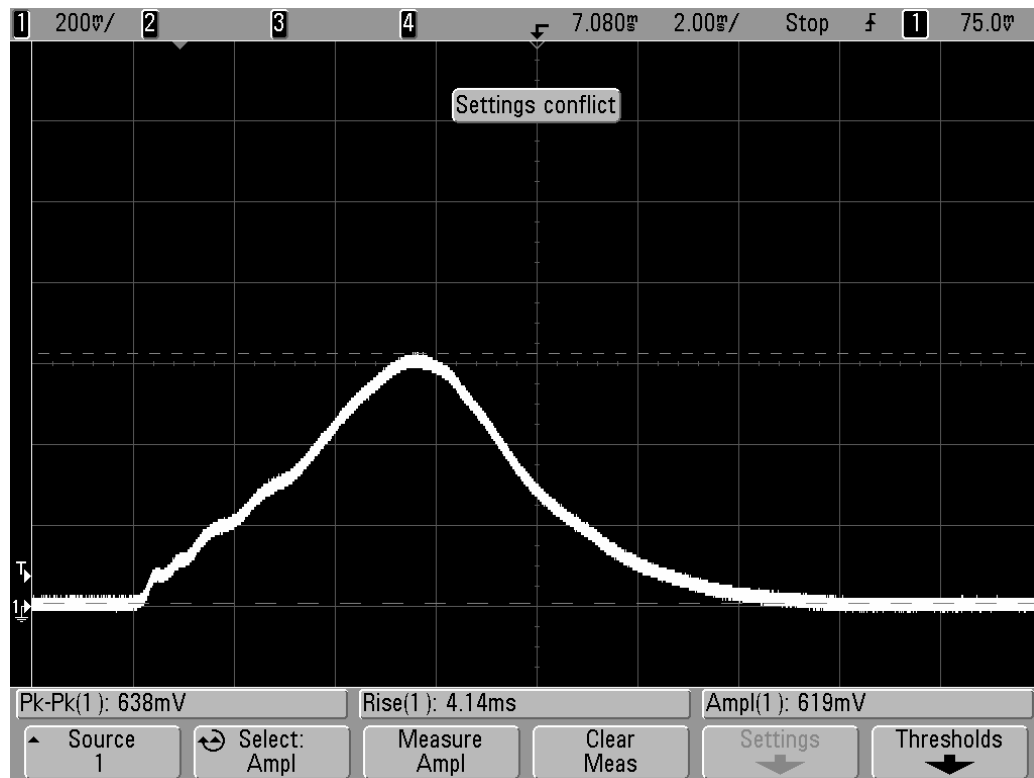
Figure 4.7. Typical force measurement for the intermediate force category.
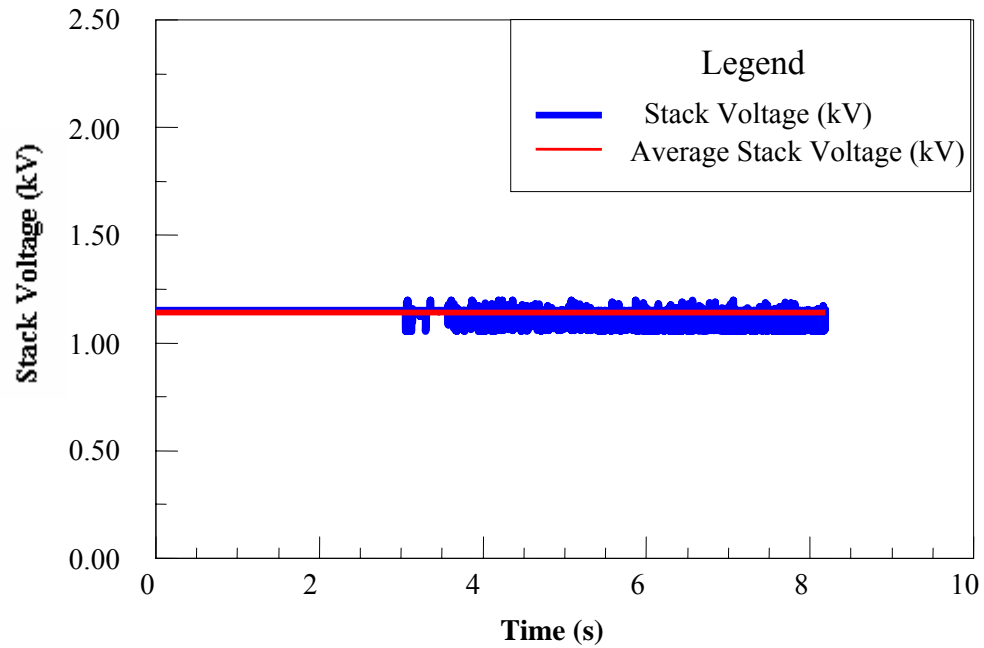
Figure 4.8. Typical voltage measurement for the intermediate force category.

The complete results for each for the intermediate force category are listed in Table 4.3. A total of 7 separate generators were tested, and five of the prototypes reached 1000 volts or higher. S/N 17 & S/N 18 both reached 1000 volts on the first and second test runs. This exceeds the specification of 1000 volts for one test. Capacitance and dissipation factor measurements were taken before and after testing, noting another increase in capacitance after the tests.

Table 4.3. Summary of the intermediate force experimental results.

Experiments		$V_{average}$ (Volts)	Force$_{peak}$ (kN)	Capacitance (nF) / Dissipation Factor
Middle Group*				
S/N 6:	Test 1	1150	11.12	157 / 0.012
	Test 2	650	9.34	
	Test 3	650	9.45	
	Test 4	690	10.68	180 / 0.017
S/N 7:	Test 1	1000	11.67	149.16 / 0.010
	Test 2	750	11.57	
	Test 3	800	12.35	
	Test 4	800	12.12	174 / 0.018
S/N 8:	Test 1	900	10.68	148.3 / 0.011
	Test 2	800	10.68	
	Test 3	800	11.35	
	Test 4	800	11.12	168.4 / 0.018
S/N 9:	Test 1	-	10.68	150.1 / 0.011
	Test 2	800	11.46	
	Test 3	750	11.57	
	Test 4	600	11.01	170.8 / 0.018
S/N 10:	Test 1	900	11.90	149.5 / 0.010
	Test 2	800	11.67	
	Test 3	780	10.91	
	Test 4	780	10.78	170.8 / 0.018
S/N 17:	Test 1	1250	10.32	149.03 / 0.011
	Test 2	1100	9.00	
	Test 3	700	9.45	
	Test 4	800	9.45	174.3 / 0.017
S/N 18:	Test 1	1000	9.79	150.6 / 0.012
	Test 2	1000	10.34	
	Test 3	800	10.23	
	Test 4	800	10.46	174.8 / 0.018

* Intermediate force group was taken to an approximate height of 1.37 m and used 8.89 cm of neoprene.

Figure 4.9 is the following result of the intermediate force test. One important observation from this figure and the prior table is S/N 17 and S/N 9 on the first test runs, were out of the range of the theoretical model. This was once again due to operator error. Another important observation of Figure 4.9 is the voltage performance of all the tests. All of the tests achieved much higher results than the theoretical model. The reason for this is the electromechanical coupling factor is much higher than specified in the manufacturer's data sheets. The next category of testing described is the high force grouping.
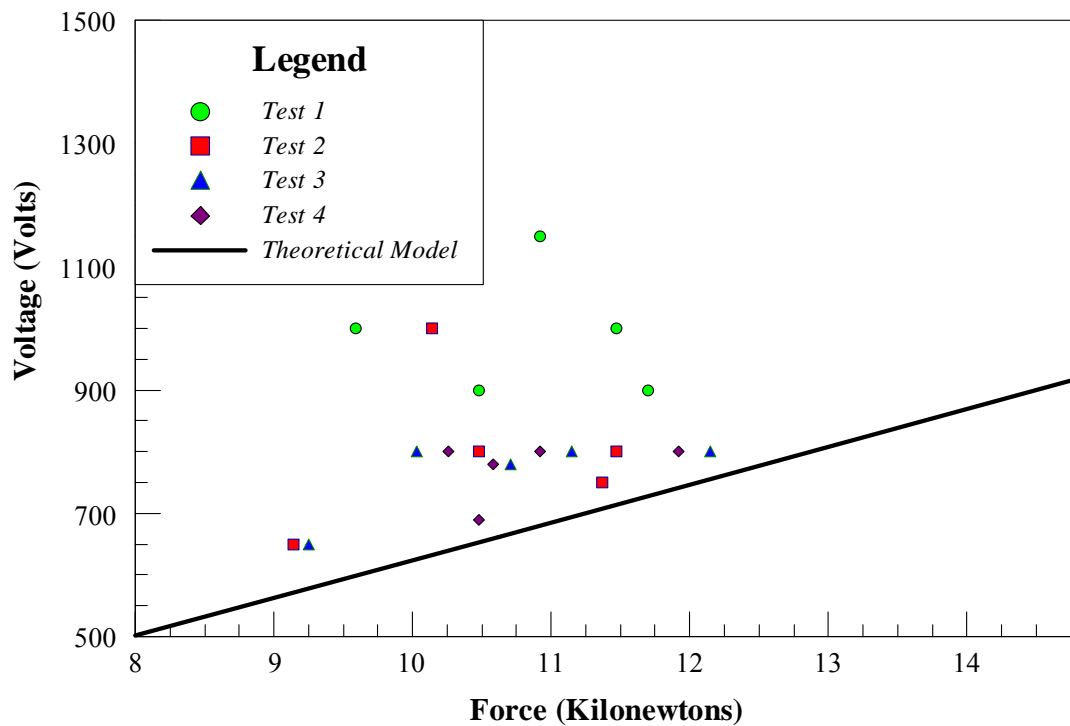

Figure 4.9. Intermediate force results.

4.4 High Force Results

The high force category uses the same experimental arrangement and testing for the low force and intermediate force. The testing procedure is discussed in Chapter 3. The high force category uses 7.62 cm of neoprene and the compression mass is released at 2.13 m. Figure 4.10 shows the typical force from the high force category. The force is around 18 kN with a 4.5 ms risetime.
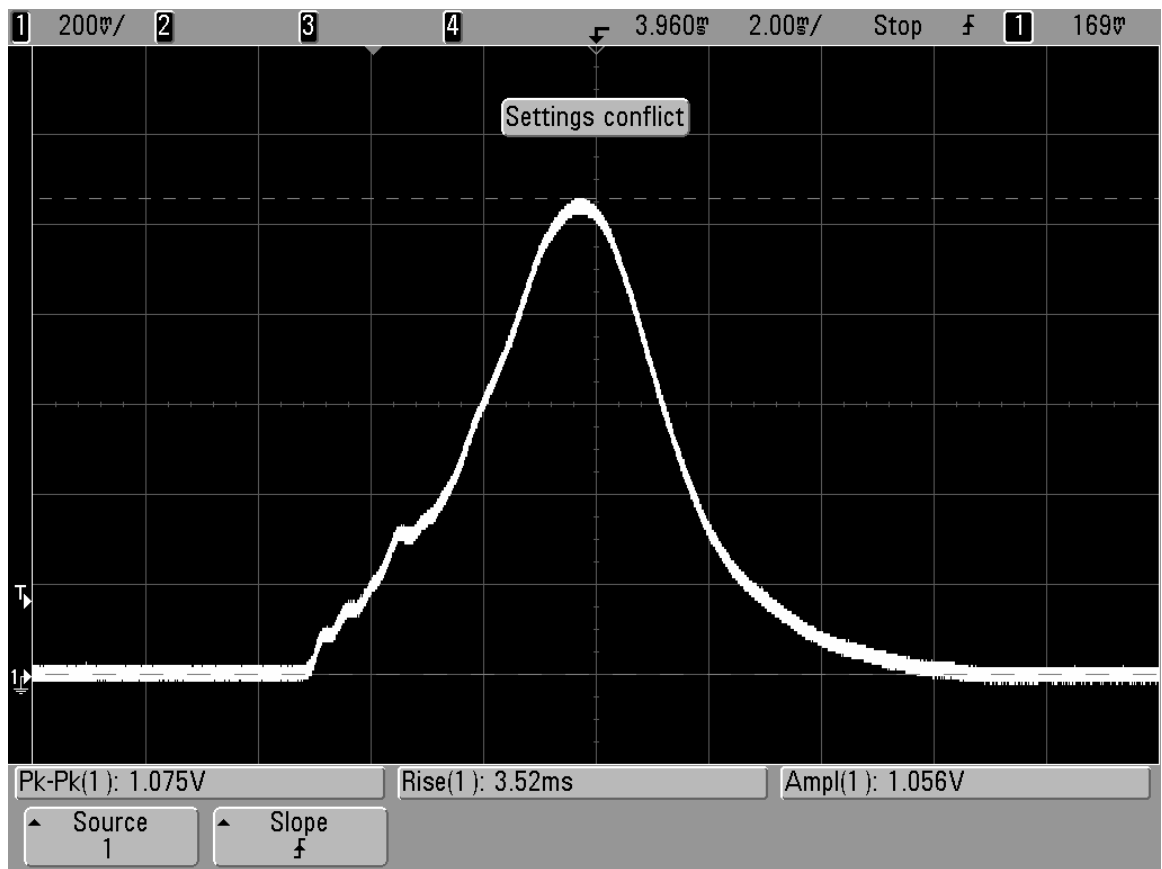

Figure 4.10. High force category typical force reading.

Figure 4.11 illustrates the typical output voltage from the high force category. The compression force used to obtain the data of Figure 4.11 is approximately 17.79 kN of force. One important characteristic to note from Figure 4.11 is the average output voltage was around 1500 volts which is much higher than the expected simulated results discussed in Chapter 2. Thus, the high force category performs at a higher level than manufacturer's anticipated results. Once again, the noise noted at the beginning of Figure 4.11 is due to the static electricity in the PVC drop height cylinder.
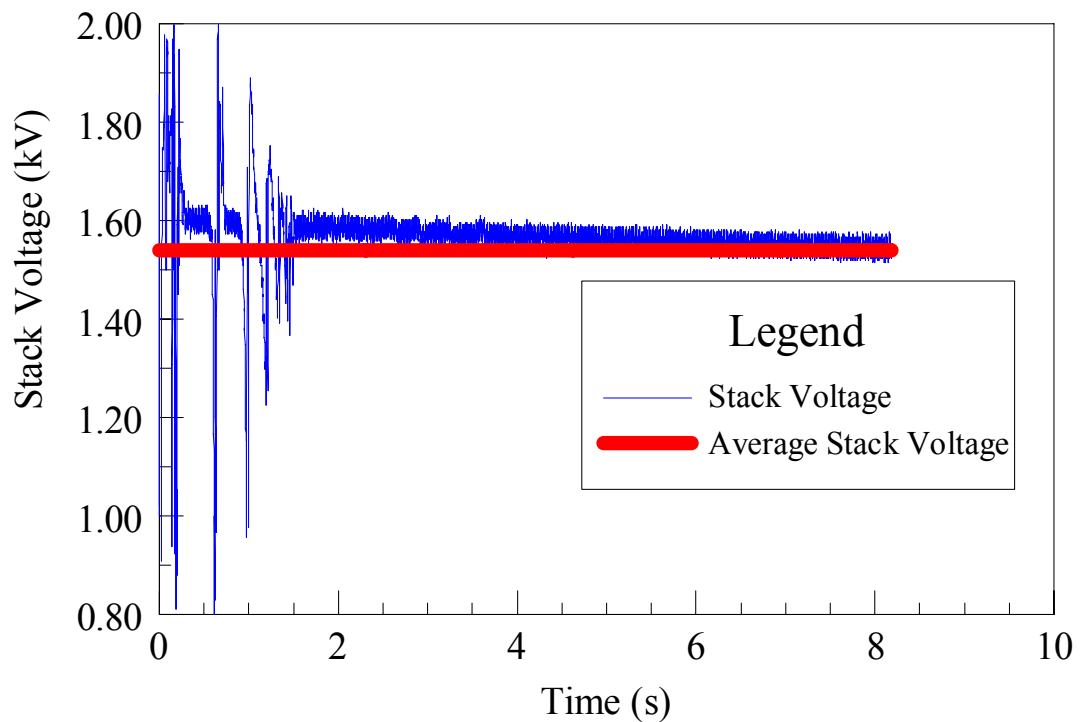

Figure 4.11. Typical measured output voltage for the high force category.

Table 4.4 lists the experimental results for the high force generators. Each generator was tested four times, with each generator breaking (mechanically) on the fourth test. Typically, the force was approximately around 18 kN although some variation in the force occurred. The variation of force was due to non-repeatability of the releasing the compression mass. An important remark to bring attention to is that the high force category was the first testing with the PZ assembled stacks. Thus, no measurements were made for the capacitance before and after testing. The highest output voltage recorded was 1540 volts on generator S/N 1. The peak force for this test was 21.35 kN.

Figure 4.12 is the high force results plotted against the theoretical model seen in Chapter 2. Once again, the high force category was the first test completed with the high energy PPG. Thus the results are not as repeatable as seen in the low force and intermediate force types. However, one of the most beneficial tests is the high force-short. The next section explains the high force- short grouping.

Table 4.4. Summary high force experimental results.

| Generator#	$V_{average}$ [V]	$Force_{peak}$ [kN]
S/N 1:		
Test 1	1540	21.35
Test 2	963	19.57
Test 3	886	18.68
Test 4	786	20.46
Test 5	Broken generator	
S/N 2:		
Test 1	1380	17.79
Test 2	1350	16.01
Test 3	938	16.01
Test 4	778	17.79
Test 5	Broken generator	
S/N 3:		
Test 1	1410	17.35
Test 2	1100	16.46
Test 3	1001	17.79
Test 4	733	17.35
Test 5	Broken generator	
S/N 4:		
Test 1	1430	16.90
Test 2	1160	14.68
Test 3	927	16.91
Test 4	784	17.79
Test 5	Broken generator	
S/N 5:		
Test 1	1390	15.12
Test 2	1070	15.84
Test 3	1190	17.44
Test 4	689	16.01
Test 5	Broken generator	
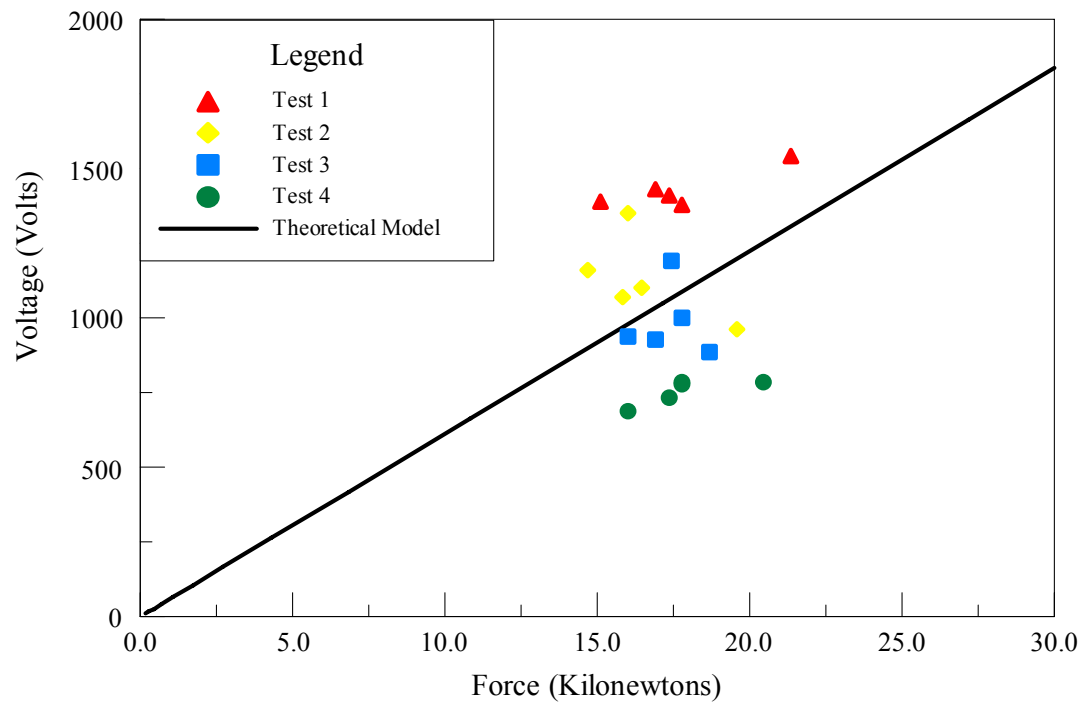
Figure 4.12. High Force Results

4.5 High Force – Short

The high force – short tests were done because a small, reverse polarity charge remained on the PZ stack even after the load capacitor was shorted. Typically, the voltage that remained on the high energy PPG was approximately -150 V. The reason for this charge is believed to be a result of the air gap capacitance created by a gap between the foils of the PZ assembled stack and the piezoelectric elements. Although the manufacturer states the piezoelectric element ends were metallized, visual inspection showed little evidence of this metallization. An example of the discharge is seen in Figure 4.13. The discharge measured to be around -150 V with a discharge time of approximately 4.5 seconds.
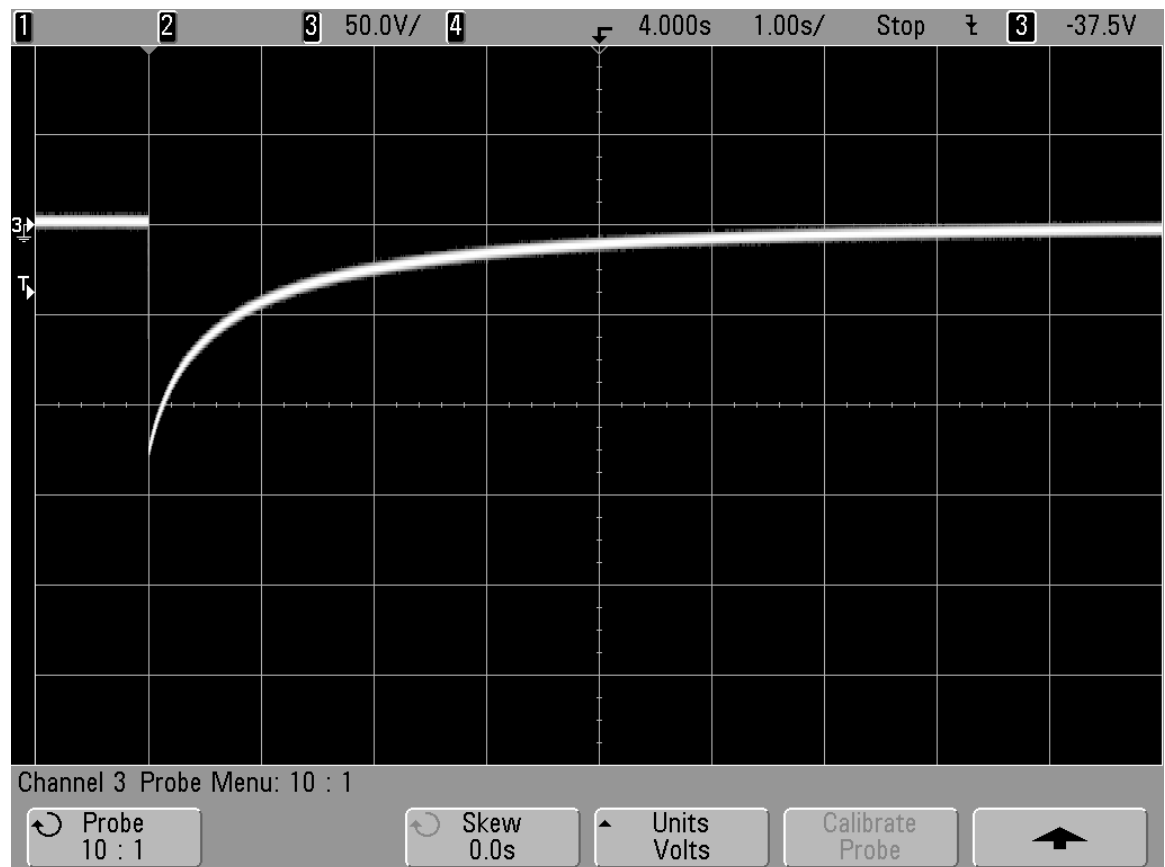

Figure 4.13. Example of observed discharge.

The high force- short test procedure is essentially the same as the high force test procedure, except that the piezoelectric elements are shorted after each test. Thus, the name high force- short category. The high force- short test used 7.62 cm of neoprene with a mass drop height of 2.134 m. The typical force profile from the high force-short test is shown in Figure 4.14. The force in that figure is 18.79 kN with a risetime of 4.4 ms. Once again, the risetime measurement is taken as the 0% - 100% point of the waveform. Figure 4.15 is a typical voltage reading from the high force- short tests. In this figure, the output voltage reached approximately 1500 volts over a 10 second period as indicated by the red line. The 1500 volts is a typical voltage reading seen in this test sequence, exceeding 1000 volts.
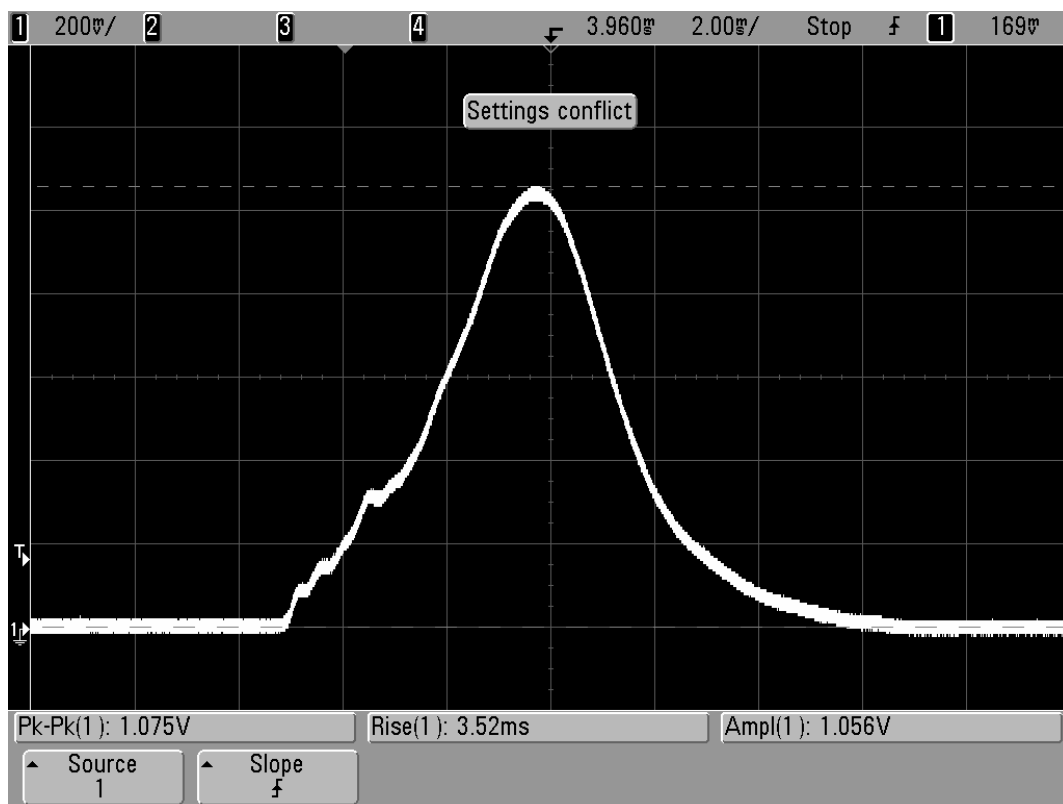

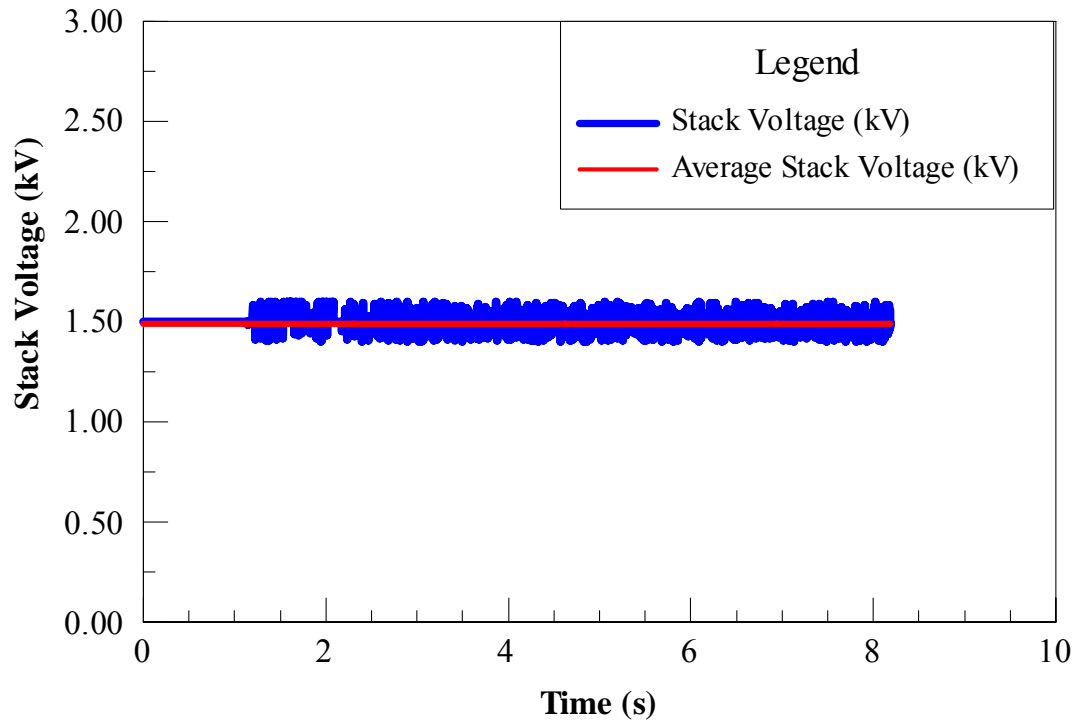Figure 4.14. Typical force measurement for the high force-short group.

Figure 4.15. Typical voltage measurement for high force – short generators.

Once again, the high force- short category testing procedures were similar to the high force category. Table 4.5 lists the test data for each of the high force- short prototype. The first test on each prototype reached around 1500 volts. Also, each individual prototype completed 4 tests, with each voltage well above the characterized 1000 volts. An increase in system's capacitance was noted for this test also.

Figure 4.16 is the high force- short results plotted against the theoretical limit. This figure demonstrates the higher than expected results for the first test run. The second, third, and fourth test results are well within the theoretical limit.

Table 4.5. Summary of high force-short experimental results.

Experiments		$V_{average}$ (Volts)	$Force_{peak}$ (kN)	Capacitance (nF) / Dissipation Factor
High Group* –Shorting between each test				
S/N 19:	Test 1	1500	18.68	148.3 / 0.011
	Test 2	1250	18.79	
	Test 3	1200	19.68	
	Test 4	1100	19.68	180.6 / 0.019
S/N 20:	Test 1	1500	18.24	151.1 / 0.012
	Test 2	1250	18.91	
	Test 3	1250	18.24	
	Test 4	1250	18.24	175.4 / 0.018
S/N 21:	Test 1	1450	18.24	148.4 / 0.011
	Test 2	1200	18.24	
	Test 3	1200	18.13	
	Test 4	1050	17.45	180 / 0.019
S/N 22:	Test 1	1500	18.24	148.4 / 0.011
	Test 2	1250	18.91	
	Test 3	1250	18.91	
	Test 4	1150	18.34	179.2 / 0.018
S/N 23:	Test 1	1500	18.68	148.5 / .011
	Test 2	1150	19.57	
	Test 3	1150	17.35	
	Test 4	1150	20.02	179.5 / .019

* High force group was taken to an approximate height of 2.134 m and used 7.62 cm of neoprene.
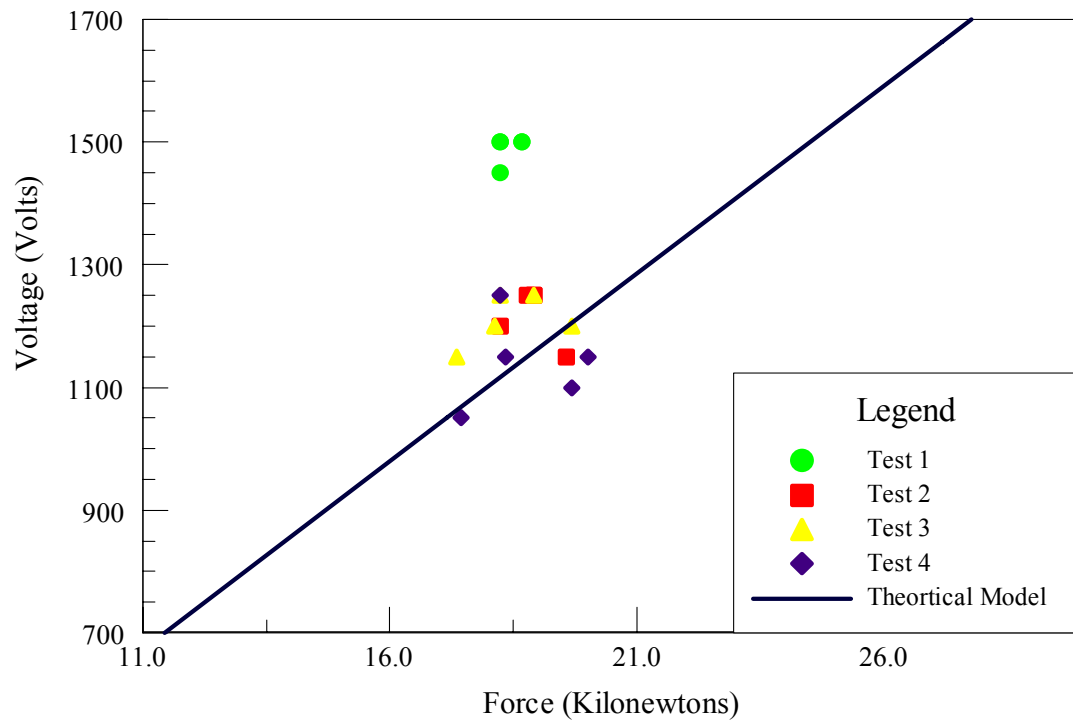
Figure 4.16. High force- short results.

4.6 Maximum Voltage

After trying to characterize the high energy PPG, there was a question to be answered on the total maximum voltage achieved by the high energy PPG. So in the maximum voltage category, tests were completed to increase the force to determine whether the voltage will also increase. The compression mass was released in the drop height cylinder from 2.34 m and the neoprene thickness is from 6.35 cm to 2.54 cm. This caused the force to vary from 23 kN to 41 kN. Testing procedures remained the same as in the previous categories. Figure 4.17 shows the force observed from one of tests. The force was measured around 33.45 kN and a rise time of around 3.5 ms. The arrow on the figure points to ground.
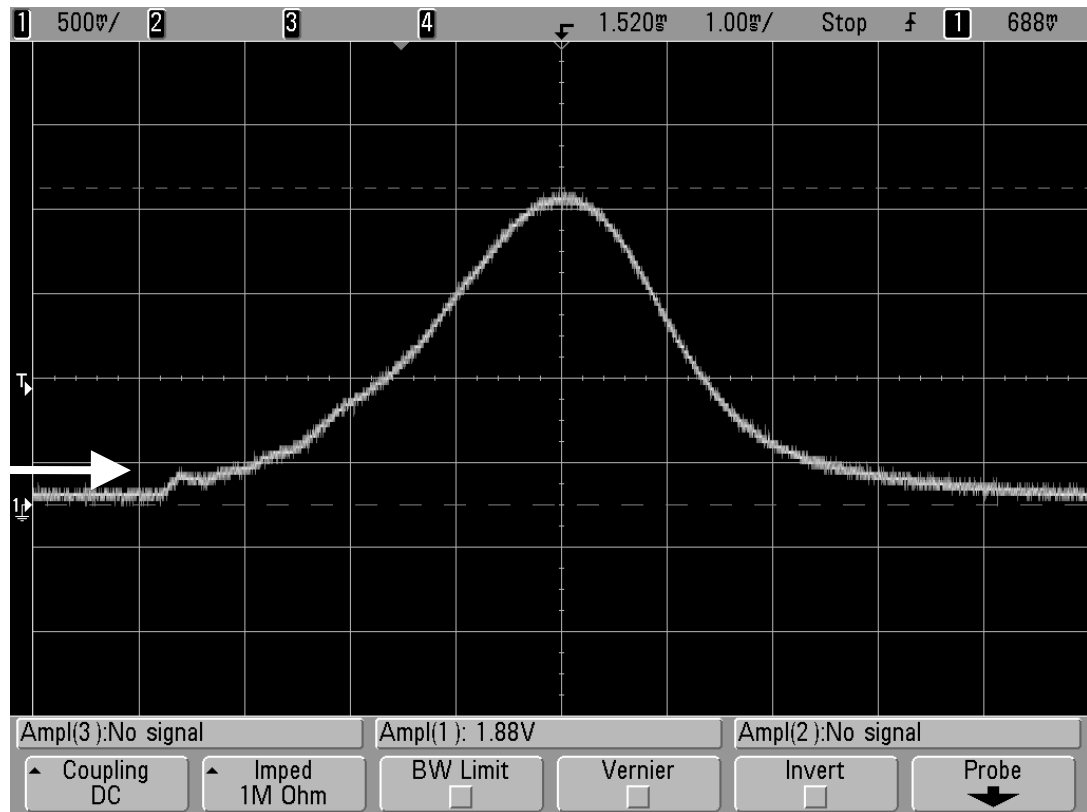

Figure 4.17. Typical force measurement for maximum voltage.

Figure 4.18 is the typical output voltage from the high energy PPG in the maximum voltage category. The average voltage was around 1450 volts with a 33 kN force over a 10 second period. The noise in the voltage reading is due to static electricity within the drop height cylinder.
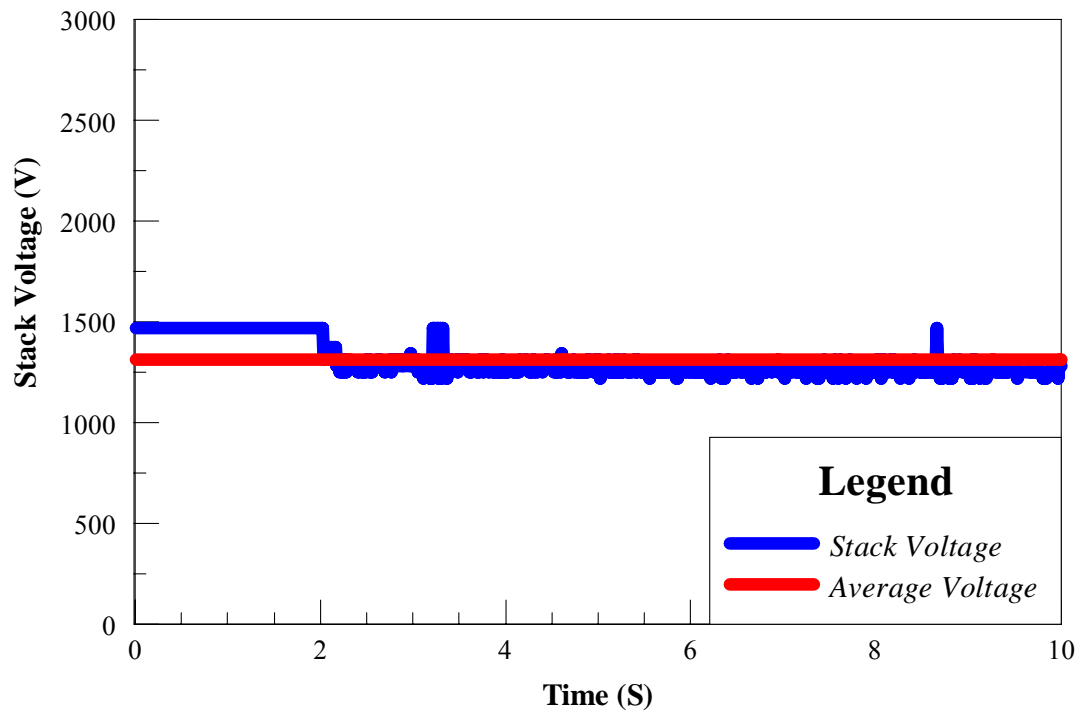

Figure 4.18. Typical output voltage measurement for maximum voltage.

Table 4.6 is the summary of the maximum voltage results. The capacitance increased on each separate PZ stack after four tests. Even though the force increased in this testing, the voltage still remained around 1500 volts, the same output voltage in the high force category.

Table 4.6. Summary of maximum voltage results.

Experiments		$V_{average}$ (Volts)	$Force_{peak}$ (kN)	Capacitance (nF) / Dissipation Factor
Maximum Voltage				
S/N 25*:	Test 1	1400	26.69	147.8 / .011
	Test 2	1250	28.11	
	Test 3	1300	26.16	
	Test 4	1050	23.84	180.1 / .020
S/N 26*:	Test 1	1520	25.80	148.3 / .011
	Test 2	1200	23.66	
	Test 3	1170	24.73	
	Test 4	1190	25.80	176.97 / .019
S/N 28**:	Test 1	1588	33.45	147.7 / .012
	Test 2	855	30.60	
	Test 3	869	35.48	
	Test 4	931	35.53	178.42 / .015
S/N 29**:	Test 1	1375	33.63	152.65 / .010
	Test 2	1160	35.23	
	Test 3	980	37.70	
	Test 4	690	27.58	172.8 / .019
S/N 30***:	Test 1	1506	39.68	148.2 / .011
	Test 2	1310	39.68	
	Test 3	1380	40.92	
	Test 4	1230	40.03	181.45 / .020

* Approximately 6.35 cm of neoprene used
**Approximately 3.81 cm of neoprene used
***Approximately 2.54 cm of neoprene used

Figure 4.19 plots all of the tests against the theoretical model in the simulation
and the resulted maximum voltage expected according to the manufacturer's, APC,
data sheets. The tests prove, the high energy PPG does not increase with an increasing
force as expected from the linear plot line of the theoretical model. Thus, the high
energy PPG can be characterized as having a maximum voltage of around 1500 volts
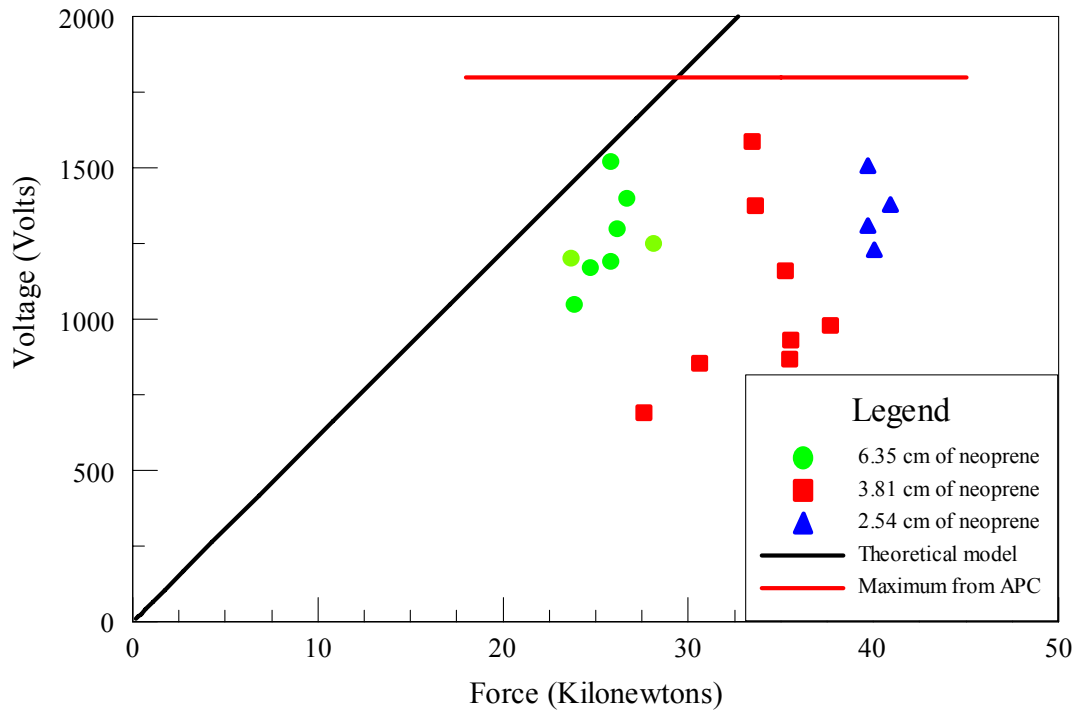despite any increase in force.

Figure 4.19. Maximum voltage results

4.7 Discussion

Figure 4.20 plots all test data contained in Tables 4.2, 4.3, 4.4, 4.5, and 4.6 along with the theoretical model predictions of output voltage discussed in Chapter 2. The data are grouped according to the test, with each test assigned a different color and symbol.
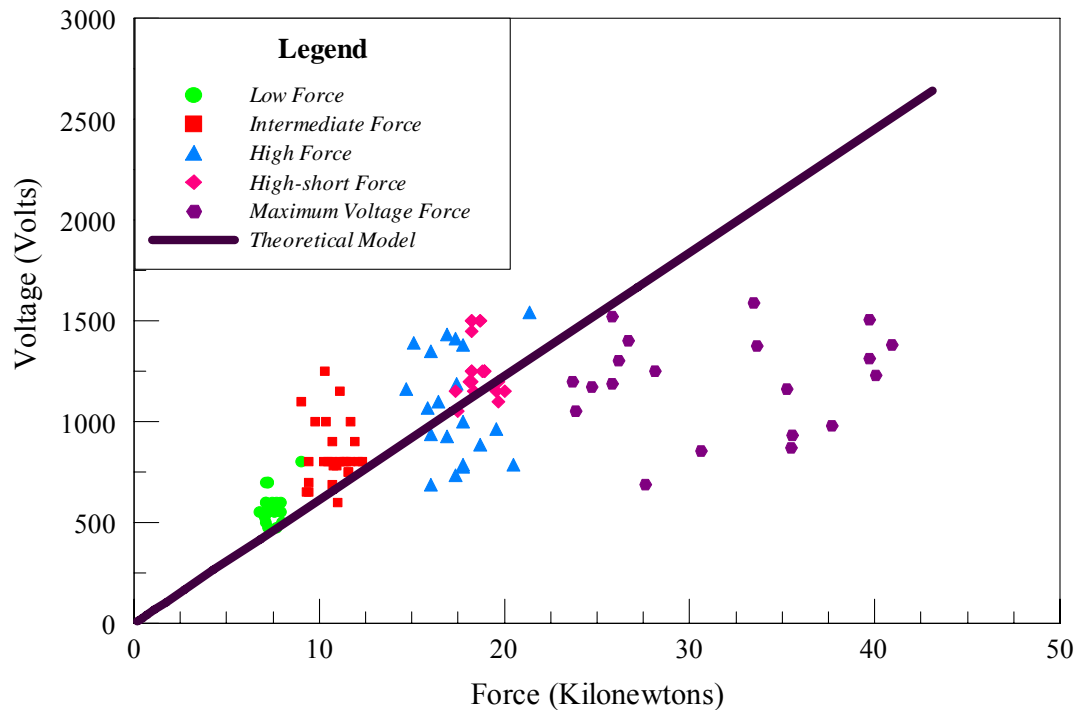

Figure 4.20. Voltage distribution compared to the theoretical model results.

Figure 4.21, however, plots the data for the first test only of the data contained in Table 4.2, 4.3, 4.4, 4.5, and 4.6 along with the theoretical model results of output voltage. Once again, the theoretical model results are discussed using PSpice in Chapter 2. In Figure 4.21, the best fit linear approximation to the measured results (i.e., lightest colored line) is given by the equation

$$V_{out} = 0.037 \times Force.$$

The theoretical predictions from the theoretical model (i.e., darkest line) are given by

$$V_{out} = 0.025 \times Force.$$

The difference between the theoretical model and the best fit linear approximation can only be a higher degree of electromechanical coupling, i.e., a higher k_{33} value. Since the manufacturer specified k_{33} value is derived from the application of a continuous, sinusoidal force, it is reasonable to think the mechanical coupling might be higher with an impact force. The maximum voltage obtained by the high energy PPG (i.e., dark horizontal line, Figure 4.21) is dependent on the poling field of 2400 V/mm. Since the PZ elements are 0.762 mm thick, the maximum voltage is approximately 1828 volts.
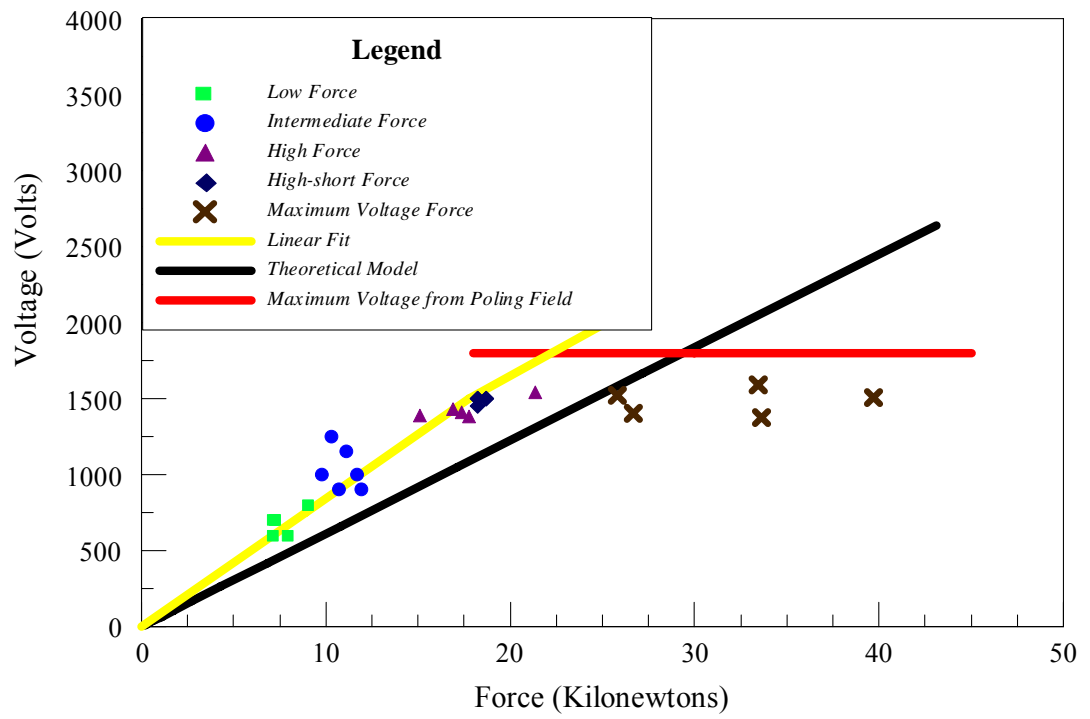
Figure 4.21. The voltage distribution compared to the theoretical model results-
Test 1 results only.

Chapter 5 Conclusion

The purpose of the high energy PPG is to charge an external 0.1 µF capacitor to 1000 V using a 18 kN force with a 5 ms risetime. The external capacitor must retain its charge voltage for a minimum time of 5 seconds. However, these requirements were met, despite the appearance of an unforeseen parasitic capacitance problem caused by manufacturing error as explained in the results. The piezoelectric assembled stack has a higher capacitance after testing because of the air gap between each piezoelectric element has a higher parasitic capacitance. In fact, the high energy PPG produced a maximum output voltage of 1588 V. So in conclusion, the high energy PPG can produced at best a maximum voltage of around 1500 V, even after increasing the force and lowering the risetime.

Data collected during this research period also appear to show that a higher degree of electromechanical coupling factor than specified by APC may exist for impact loads. Although project requirements did not specify a multi-shot lifetime for the prototype generators, tests were performed to determine the lifetime high energy PPGs. Generally, the high energy PPG lasted for around 4 tests in each run. The four test characterization was demonstrated since there was a piezoelectric stack degradation after the first test. This degradation is seen as a drop in the voltage after the first test. Although mechanical breakage occurred in testing, depolarization of the PZ was thought to be the limiting factor affecting lifetime.

REFERENCES

[1] C. Keawboonchuay, "*Investigation and optimization of a piezoelectric pulse generator.*" Doctor's Dissertation, University of Missouri- Columbia, December 2003.

[2] Morgan Matroc, Inc., 225 Theodore Rice Blvd., New Bedford, MA 02745.

[3] S.Platt, S. Farritor, and H. Haider, "On low- frequency electric power generation with PZT ceramics," *IEEE Trans. Mechatronics.*, vol. 10, No. 2, pp. 240-245, April 2005.

[4] C. Keawboonchuay, and T.G. Engel, "Design, modeling, and implementation of a 30-kW piezoelectric pulse generator," *IEEE Trans. Plasma Science*, vol. 30, No.2, pp. 679-686, April 2002.

[5] C. Keawboonchuay, and T.G. Engel, "Electrical power generation characteristics of piezoelectric generator under quasi-static and dynamic stress conditions," *IEEE Trans. Ultrasonics, Ferroelectrics, and Frequency Control*, vol. 50, No.10, pp. 1377-1382, October 2003.

[6] C. Keawboonchuay, and T.G. Engel, "Maximum power generation in a piezoelectric pulse generator," *IEEE Trans. Plasma Science*, vol. 31, No. 1, pp. 123-128, February 2003.

[7] C. Pinkston, and T.G. Engel, "High energy and piezoelectric pulse generator," *IEEEPulsed Power Conference*, 2005.

[8] M. Duffy, and D. Carroll, "Electromagnetic generators for power harvesting," in *Proc. IEEE Power Electronics Specialists Conference*, 2004, pp. 2075-2081.

[9] S.S. Rao, *Mechanical Vibrations*. Reading, MA, 1986, pp. 261-320.

[10] Agilent Technology. 395 Page Mill Rd., P.O. Box #10395, Palo Alto, CA 94303.

[11] American Piezo Ceramics, Inc., Duck Run, P.O. Box 180 Mackeyville, PA 17750.

[12] OrCAD PSpice A/D, version 9.3, OrCAD, Inc., 9300 SW Nimbus Ave., Beaverton, OR 97008, 2001.

[13] PCB Piezotronics, Inc., 3425 Walden Avenue, Depew, NY 14043.